

Dilaton Interactions and the Anomalous Breaking of Scale Invariance of the Standard Model

Claudio Corianò, Luigi Delle Rose, Antonio Quintavalle and Mirko Serino

Dipartimento di Matematica e Fisica "Ennio De Giorgi"

Università del Salento

and

INFN-Lecce

Via Arnesano 73100, Lecce, Italy¹

Abstract

We discuss the main features of dilaton interactions for fundamental and effective dilaton fields. In particular, we elaborate on the various ways in which dilatons can couple to the Standard Model and on the role played by the conformal anomaly as a way to characterize their interactions. In the case of a dilaton derived from a metric compactification (graviscalar), we present the structure of the radiative corrections to its decay into two photons, a photon and a Z , two Z gauge bosons and two gluons, together with their renormalization properties. We prove that, in the electroweak sector, the renormalization of the theory is guaranteed only if the Higgs is conformally coupled. For such a dilaton, its coupling to the trace anomaly is quite general, and determines, for instance, an enhancement of its decay rates into two photons and two gluons. We then turn our attention to theories containing a non-gravitational (effective) dilaton, which, in our perturbative analysis, manifests as a pseudo-Nambu Goldstone mode of the dilatation current (J_D). The infrared coupling of such a state to the two-photons and to the two-gluons sector, and the corresponding anomaly enhancements of its decay rates in these channels, is critically analyzed.

¹claudio.coriano@unisalento.it, luigi.dellerose@le.infn.it, antonio.quintavalle@le.infn.it, mirko.serino@le.infn.it

1 Introduction

Dilaton is part of the low energy effective action of several different types of theories, from string theory to theories with compactified extra dimensions, but they may appear also in appropriate bottom-up constructions. For instance, in scale-invariant extensions of the Standard Model, the introduction of a dilaton field allows to recover scale invariance, which is violated by the Higgs potential, by introducing a new, enlarged, Lagrangian. This is characterized both by a spontaneous breaking of the conformal and of the electroweak symmetries.

In this case, one can formulate simple scale-invariant extensions of the potential which can accommodate, via spontaneous breakings, two separate scales: the electroweak scale (v), related to the vev of the Higgs field, and the conformal breaking scale (Λ), related to the vev of a new field $\Sigma = \Lambda + \rho$, with ρ being the dilaton. The second scale can be fine-tuned in order to proceed with a direct phenomenological analysis and is, therefore, of outmost relevance in the search for new physics at the LHC.

In a bottom-up approach, and this will be one of the main points that we will address in our analysis, the dilaton of the effective scale-invariant Lagrangian can also be interpreted as a composite scalar, with the dilatation current taking the role of an operator which interpolates between this state and the vacuum. We will relate this interpretation to the appearance of an anomaly pole in the correlation function involving the dilatation current (J_D) and two neutral currents (V, V') of the Standard Model, providing evidence, in the ordinary perturbative picture, in favour of such a statement.

One of the main issues which sets a difference between the various types of dilatons is, indeed, the contribution coming from the anomaly, which is expected to be quite large. Dilatons obtained from compactifications with large extra dimensions and a low gravity scale, for instance, carry this coupling, which is phenomenologically relevant. The same coupling is present in the case of an effective dilaton, appearing as a Goldstone mode of the dilatation current, with some differences that we will specify in a second part of our work. The analysis will be carried out in analogy to the pion case, which in a perturbative picture is associated with the appearance of an anomaly pole in the AVV diagram (with A being the axial current).

Our work is organized as follows. In a first part we will characterize the leading one-loop interactions of a dilaton derived from a Kaluza-Klein compactification of the gravitational metric. The setup is analogous to that presented in [1, 2] for a compactified theory with large extra dimensions and it involves all the neutral currents of the Standard Model. We present also a discussion of the same interaction in the QCD case for off-shell gluons.

These interactions are obtained by tracing the TVV' vertex, with T denoting the (symmetric and conserved) energy-momentum tensor (EMT) of the Standard Model. This study is accompanied by an explicit proof of the renormalizability of these interactions in the case of a conformally coupled Higgs scalar.

In a second part then we turn our discussion towards models in which dilatons are introduced from the ground up, starting with simple examples which should clarify - at least up to operators of dimension 4 - how one can proceed with the formulation of scale-invariant extensions of the Standard Model. Some of the more technical material concerning this point has been left to the appendices, where we illustrate the nature of the coupling of the dilaton to the mass dependent terms of the corresponding Lagrangian. The goal of these technical additions is to clarify that a fundamental (i.e. not a composite) dilaton, in a *classical* scale invariant extension of a given Lagrangian, does not necessarily couple to the anomaly, but only to massive states, exactly

as in the Higgs case. For an effective dilaton, instead, the Lagrangian is derived at tree level on the basis of classical scale invariance, as for a fundamental dilaton, which needs to be modified with the addition of an anomalous contribution, due to the composite nature of the scalar, in close analogy to the pion case.

As we are going to show, if the dilaton is a composite state, identified with the anomaly pole of the $J_D VV$ correlator, an infrared coupling of this pole (i.e. a nonzero residue) is necessary in order to claim the presence of an anomaly enhancement in the VV decay channel, with the VV denoting on-shell physical asymptotic states, in a typical S -matrix approach. Here our reasoning follows quite closely the chiral anomaly case, where the anomaly pole of the AVV diagram, which describes the pion exchange between the axial vector (A) and the vector currents, is infrared coupled only if V denote physical asymptotic states.

Clearly, our argument relies on a perturbative picture and is, in this respect, admittedly limited, forcing this issue to be resolved at experimental level, as in the pion case. We recall that in the pion the enhancement is present in the di-photon channel and not in the 2-gluon decay channel.

Perturbation theory, in any case, allows to link the enhancement of a certain dilaton production/decay channel, to the virtuality of the gauge currents in the initial or the final state.

We conclude with a discussion of the possible phenomenological implications of our results at the level of anomaly-enhanced dilaton decays, after pointing out the difference between the various ways in which the requirement of scale invariance (classical or quantum) can be realized in a typical scale-invariant extension of the Standard Model Lagrangian.

1.1 The energy momentum tensor

We start with a brief summary of the structure of the Standard Model interactions with a $4D$ gravitational background, which is convenient in order to describe both the coupling of the graviscalar dilaton, emerging from the Kaluza-Klein compactification, and of a graviton at tree level and at higher orders. In the background metric $g_{\mu\nu}$ the action takes the form

$$S = S_G + S_{SM} + S_I = -\frac{1}{\kappa^2} \int d^4x \sqrt{-g} R + \int d^4x \sqrt{-g} \mathcal{L}_{SM} + \chi \int d^4x \sqrt{-g} R H^\dagger H, \quad (1)$$

where $\kappa^2 = 16\pi G_N$, with G_N being the four dimensional Newton's constant and \mathcal{H} is the Higgs doublet. We recall that the EMT in our conventions is defined as

$$T_{\mu\nu}(x) = \frac{2}{\sqrt{-g(x)}} \frac{\delta[S_{SM} + S_I]}{\delta g^{\mu\nu}(x)}, \quad (2)$$

or, in terms of the SM Lagrangian, as

$$\frac{1}{2} \sqrt{-g} T_{\mu\nu} \equiv \frac{\partial(\sqrt{-g} \mathcal{L})}{\partial g^{\mu\nu}} - \frac{\partial}{\partial x^\sigma} \frac{\partial(\sqrt{-g} \mathcal{L})}{\partial(\partial_\sigma g^{\mu\nu})}, \quad (3)$$

which is classically covariantly conserved ($g^{\mu\rho} T_{\mu\nu;\rho} = 0$). In flat spacetime, the covariant derivative is replaced by the ordinary derivative, giving the ordinary conservation equation ($\partial_\mu T^{\mu\nu} = 0$).

We use the convention $\eta_{\mu\nu} = (1, -1, -1, -1)$ for the metric in flat spacetime, parameterizing its deviations from the flat case as

$$g_{\mu\nu}(x) \equiv \eta_{\mu\nu} + \kappa h_{\mu\nu}(x), \quad (4)$$

with the symmetric rank-2 tensor $h_{\mu\nu}(x)$ accounting for its fluctuations.

In this limit, the coupling of the Lagrangian to gravity is given by the term

$$\mathcal{L}_{grav}(x) = -\frac{\kappa}{2}T^{\mu\nu}(x)h_{\mu\nu}(x). \quad (5)$$

In the case of theories with extra spacetime dimensions the structure of the corresponding Lagrangian can be found in [1, 2]. For instance, in the case of a compactification over a S_1 circle of a 5-dimensional theory to 4D, equation (5) is modified in the form

$$\mathcal{L}_{grav}(x) = -\frac{\kappa}{2}T^{\mu\nu}(x)(h_{\mu\nu}(x) + \rho(x)\eta_{\mu\nu}) \quad (6)$$

which is sufficient in order to describe dilaton (ρ) interactions with the fields of the Standard Model at leading order in κ , as in our case. In this case the graviscalar field ρ is related to the g_{55} component of the 5D metric and describes its massless Kaluza-Klein mode. The compactification generates an off-shell coupling of ρ to the trace of the symmetric EMT. Notice that in this construction the fermions are assumed to live on the 4D brane and their interactions can be described by the ordinary embedding of the fermionic Lagrangian of the Standard Model to a curved 4D gravitational background. We use the spin connection Ω induced by the curved metric $g_{\mu\nu}$. This allows to define a spinor derivative \mathcal{D} which transforms covariantly under local Lorentz transformations. If we denote with $\underline{a}, \underline{b}$ the Lorentz indices of a local free-falling frame, and denote with $\sigma^{\underline{ab}}$ the generators of the Lorentz group in the spinorial representation, the spin connection takes the form

$$\Omega_\mu(x) = \frac{1}{2}\sigma^{\underline{ab}}V_{\underline{a}}^\nu(x)V_{\underline{b}\nu;\mu}(x), \quad (7)$$

where we have introduced the vielbein $V_{\underline{a}}^\mu(x)$. The covariant derivative of a spinor in a given representation (R) of the gauge symmetry group, expressed in curved (\mathcal{D}_μ) coordinates is then given by

$$\mathcal{D}_\mu = \frac{\partial}{\partial x^\mu} + \Omega_\mu + A_\mu, \quad (8)$$

where $A_\mu \equiv A_\mu^a T^{a(R)}$ are the gauge fields and $T^{a(R)}$ the group generators, giving a Lagrangian of the form

$$\mathcal{L} = \sqrt{-g} \left\{ \frac{i}{2} \left[\bar{\psi} \gamma^\mu (\mathcal{D}_\mu \psi) - (\mathcal{D}_\mu \bar{\psi}) \gamma^\mu \psi \right] - m \bar{\psi} \psi \right\}. \quad (9)$$

The derivation of the complete dilaton/gauge/gauge vertex in the Standard Model requires the computation of the trace of the EMT $T^\mu{}_\mu$ (for the tree-level contributions), and of a large set of 1-loop 3-point functions. These are diagrams characterized by the insertion of the trace into 2-point functions of gauge currents. The full EMT is given by a minimal tensor $T_{Min}^{\mu\nu}$ (without improvement) and by a term of improvement, $T_I^{\mu\nu}$, originating from S_I , as

$$T^{\mu\nu} = T_{Min}^{\mu\nu} + T_I^{\mu\nu}, \quad (10)$$

where the minimal tensor is decomposed into gauge, ghost, Higgs, Yukawa and gauge fixing (g.fix.) contributions which can be found in [3]

$$T_{Min}^{\mu\nu} = T_{gauge}^{\mu\nu} + T_{ferm.}^{\mu\nu} + T_{Higgs}^{\mu\nu} + T_{Yukawa}^{\mu\nu} + T_{g.fix.}^{\mu\nu} + T_{ghost}^{\mu\nu}. \quad (11)$$

Concerning the structure of the EMT of improvement, we introduce the ordinary parametrizations of the Higgs field

$$H = \begin{pmatrix} -i\phi^+ \\ \frac{1}{\sqrt{2}}(v + h + i\phi) \end{pmatrix} \quad (12)$$

and of its conjugate H^\dagger , expressed in terms of h , ϕ and ϕ^\pm , corresponding to the physical Higgs and the Goldstone bosons of the Z and W^\pm respectively. As usual, v denotes the Higgs vacuum expectation value. This expansion generates a non-vanishing EMT, induced by S_I , given by

$$T_I^{\mu\nu} = -2\chi(\partial^\mu\partial^\nu - \eta^{\mu\nu}\square)H^\dagger H = -2\chi(\partial^\mu\partial^\nu - \eta^{\mu\nu}\square)\left(\frac{h^2}{2} + \frac{\phi^2}{2} + \phi^+\phi^- + v h\right). \quad (13)$$

Notice that this term is generated by a Lagrangian which does not survive the flat spacetime limit. We are going to show by an explicit computation that T_I , if properly included with $\chi = 1/6$, guarantees the renormalizability of the model.

2 One loop electroweak corrections to dilaton-gauge-gauge vertices

In this section we will present results for the structure of the radiative corrections to the dilaton/gauge/gauge vertices in the case of two photons, photon/ Z and ZZ gauge currents. We have included in Appendix D the list of the relevant tree level interactions extracted from the SM Lagrangian introduced above and which have been used in the computation of these corrections. We identify three classes of contributions, denoted as \mathcal{A} , Σ and Δ , with the \mathcal{A} -term coming from the conformal anomaly while the Σ and Δ terms are related to the exchange of fermions, gauge bosons and scalars (Higgs/Goldstones). The separation between the anomaly part and the remaining terms is typical of the TVV' interaction. In particular one can check that in a mass-independent renormalization scheme, such as Dimensional Regularization with minimal subtraction, this separation can be verified at least at one loop level and provides a realization of the (anomalous) conformal Ward identity

$$\Gamma^{\alpha\beta}(z, x, y) \equiv \eta_{\mu\nu} \left\langle T^{\mu\nu}(z) V^\alpha(x) V^\beta(y) \right\rangle = \frac{\delta^2 \mathcal{A}(z)}{\delta A_\alpha(x) \delta A_\beta(y)} + \left\langle T^\mu{}_\mu(z) V^\alpha(x) V^\beta(y) \right\rangle, \quad (14)$$

where we have denoted by $\mathcal{A}(z)$ the anomaly and A_α the gauge sources coupled to the current V^α . Notice that in the expression above $\Gamma^{\alpha\beta}$ denotes a generic dilaton/gauge/gauge vertex, which is obtained from the TVV' vertex by tracing the spacetime indices $\mu\nu$. A simple way to test the validity of (14) is to compute the renormalized vertex $\langle T^{\mu\nu} V^\alpha V'^\beta \rangle$ (i.e. the graviton/gauge/gauge vertex) and perform afterwards its 4-dimensional trace. This allows to identify the left-hand-side of this equation. On the other hand, the insertion of the trace of $T^{\mu\nu}$ (i.e. $T^\mu{}_\mu$) into a two point function VV' , allows to identify the second term on the right-hand-side of (14), $\langle T^\mu{}_\mu(z) V^\alpha(x) V^\beta(y) \rangle$. The difference between the two terms so computed can be checked to correspond to the \mathcal{A} -term, obtained by two differentiations of the anomaly functional \mathcal{A} . We recall that, in general, when scalars are conformally coupled, this takes the form

$$\mathcal{A}(z) = \sum_i \frac{\beta_i}{2g_i} F_i^{\alpha\beta}(z) F_{\alpha\beta}^i(z) + \dots, \quad (15)$$

where β_i are clearly the mass-independent β functions of the gauge fields and g_i the corresponding coupling constants, while the ellipsis refer to curvature-dependent terms. We present explicit results starting for the $\rho V V'$ vertices ($V, V' = \gamma, Z$), denoted as $\Gamma_{VV'}^{\alpha\beta}$, which are decomposed in momentum space in the form

$$\Gamma_{VV'}^{\alpha\beta}(k, p, q) = (2\pi)^4 \delta(k - p - q) \frac{i}{\Lambda} \left(\mathcal{A}^{\alpha\beta}(p, q) + \Sigma^{\alpha\beta}(p, q) + \Delta^{\alpha\beta}(p, q) \right), \quad (16)$$

where

$$\mathcal{A}^{\alpha\beta}(p, q) = \int d^4x d^4y e^{ip \cdot x + iq \cdot y} \frac{\delta^2 \mathcal{A}(0)}{\delta A^\alpha(x) \delta A^\beta(y)} \quad (17)$$

and

$$\Sigma^{\alpha\beta}(p, q) + \Delta^{\alpha\beta}(p, q) = \int d^4x d^4y e^{ip \cdot x + iq \cdot y} \left\langle T^\mu{}_\mu(0) V^\alpha(x) V^\beta(y) \right\rangle. \quad (18)$$

We have denoted with $\Sigma^{\alpha\beta}$ the cut vertex contribution to $\Gamma_{\rho V V'}^{\alpha\beta}$, while $\Delta^{\alpha\beta}$ includes the dilaton-Higgs mixing on the dilaton line, as shown in Fig. 3. Notice that $\Sigma^{\alpha\beta}$ and $\Delta^{\alpha\beta}$ take contributions in two cases, specifically if the theory has an explicit (mass dependent) breaking and/or if the scalar - which in this case is the Higgs field - is not conformally coupled. The $\mathcal{A}^{\alpha\beta}(p, q)$ represents the conformal anomaly while Λ is dilaton interaction scale.

2.1 The $\rho\gamma\gamma$ vertex

The interaction between a dilaton and two photons is identified by the diagrams in Figs. 1,2,3 and is summarized by the expression

$$\Gamma_{\gamma\gamma}^{\alpha\beta}(p, q) = \frac{i}{\Lambda} \left[\mathcal{A}^{\alpha\beta}(p, q) + \Sigma^{\alpha\beta}(p, q) + \Delta^{\alpha\beta}(p, q) \right], \quad (19)$$

with the anomaly contribution given by

$$\mathcal{A}^{\alpha\beta} = \frac{\alpha}{\pi} \left[-\frac{2}{3} \sum_f Q_f^2 + \frac{5}{2} + 6\chi \right] u^{\alpha\beta}(p, q) \stackrel{\chi \rightarrow \frac{1}{6}}{=} -2 \frac{\beta_e}{e} u^{\alpha\beta}(p, q), \quad (20)$$

where

$$u^{\alpha\beta}(p, q) = (p \cdot q) \eta^{\alpha\beta} - q^\alpha p^\beta, \quad (21)$$

and the explicit scale-breaking term $\Sigma^{\alpha\beta}$ which splits into

$$\Sigma^{\alpha\beta}(p, q) = \Sigma_F^{\alpha\beta}(p, q) + \Sigma_B^{\alpha\beta}(p, q) + \Sigma_I^{\alpha\beta}(p, q). \quad (22)$$

We obtain for the on-shell photon case ($p^2 = q^2 = 0$)

$$\begin{aligned} \Sigma_F^{\alpha\beta}(p, q) &= \frac{\alpha}{\pi} \sum_f Q_f^2 m_f^2 \left[\frac{4}{s} + 2 \left(\frac{4m_f^2}{s} - 1 \right) \mathcal{C}_0(s, 0, 0, m_f^2, m_f^2, m_f^2) \right] u^{\alpha\beta}(p, q), \\ \Sigma_B^{\alpha\beta}(p, q) &= \frac{\alpha}{\pi} \left[6M_W^2 \left(1 - 2 \frac{M_W^2}{s} \right) \mathcal{C}_0(s, 0, 0, M_W^2, M_W^2, M_W^2) - 6 \frac{M_W^2}{s} - 1 \right] u^{\alpha\beta}(p, q), \\ \Sigma_I^{\alpha\beta}(p, q) &= \frac{\alpha}{\pi} 6\chi \left[2M_W^2 \mathcal{C}_0(s, 0, 0, M_W^2, M_W^2, M_W^2) u^{\alpha\beta}(p, q) \right. \\ &\quad \left. - M_W^2 \frac{s}{2} \mathcal{C}_0(s, 0, 0, M_W^2, M_W^2, M_W^2) \eta^{\alpha\beta} \right], \end{aligned} \quad (23)$$

while the mixing contributions are given by

$$\begin{aligned}
\Delta^{\alpha\beta}(p, q) &= \frac{\alpha}{\pi(s - M_H^2)} 6\chi \left\{ 2 \sum_f Q_f^2 m_f^2 \left[2 + (4m_f^2 - s) \mathcal{C}_0(s, 0, 0, m_f^2, m_f^2, m_f^2) \right] \right. \\
&+ M_H^2 + 6M_W^2 + 2M_W^2(M_H^2 + 6M_W^2 - 4s) \mathcal{C}_0(s, 0, 0, M_W^2, M_W^2, M_W^2) \left. \right\} u^{\alpha\beta}(p, q) \\
&+ \frac{\alpha}{\pi} 3\chi s M_W^2 \mathcal{C}_0(s, 0, 0, M_W^2, M_W^2, M_W^2) \eta^{\alpha\beta}, \tag{24}
\end{aligned}$$

with α the fine structure constant. The scalar integrals are defined in Appendix E. The Σ 's and Δ terms are the contributions obtained from the insertion on the photon 2-point function of the trace of the EMT, $T^\mu{}_\mu$. Notice that Σ_I includes all the trace insertions which originate from the terms of improvement T_I except for those which are bilinear in the Higgs-dilaton fields and which have been collected in Δ . The analysis of the Ward and Slavnov-Taylor identities for the graviton-vector-vector correlators shows that these can be consistently solved only if we include the graviton-Higgs mixing on the graviton line.

We have included contributions proportional both to fermions (F) and boson (B) loops, beside the Σ_I . A conformal limit on these contributions can be performed by sending to zero all the mass terms, which is equivalent to sending the vev v to zero and requiring a conformal coupling of the Higgs ($\chi = 1/6$). In the $v \rightarrow 0$ limit, but for a generic parameter χ , we obtain

$$\lim_{v \rightarrow 0} (\Sigma^{\alpha\beta} + \Delta^{\alpha\beta}) = \lim_{v \rightarrow 0} (\Sigma_B^{\alpha\beta} + \Sigma_I^{\alpha\beta}) = \frac{\alpha}{\pi} (6\chi - 1) u^{\alpha\beta}(p, q), \tag{25}$$

which, in general, is non-vanishing. Notice that, among the various contributions, only the exchange of a boson or the term of improvement contribute in this limit and their sum vanishes only if the Higgs is conformally coupled ($\chi = \frac{1}{6}$).

Finally, we give the decay rate of the dilaton into two on-shell photons in the simplified case in which we remove the term of improvement by sending $\chi \rightarrow 0$

$$\Gamma(\rho \rightarrow \gamma\gamma) = \frac{\alpha^2 m_\rho^3}{256 \Lambda^2 \pi^3} \left| \beta_2 + \beta_Y - [2 + 3x_W + 3x_W(2 - x_W)f(x_W)] + \frac{8}{3} x_t [1 + (1 - x_t)f(x_t)] \right|^2, \tag{26}$$

where the contributions to the decay, beside the anomaly term, come from the W and the fermion (top) loops and $\beta_2 (= 19/6)$ and $\beta_Y (= -41/6)$ are the $SU(2)$ and $U(1)$ β functions respectively. Here, as well as in the other decay rates evaluated all through the paper, the x_i are defined as

$$x_i = \frac{4m_i^2}{m_\rho^2}, \tag{27}$$

with the index "i" labelling the corresponding massive particle, and x_t denoting the contribution from the top quark, which is the only massive fermion running in the loop. The function $f(x)$ is given by

$$f(x) = \begin{cases} \arcsin^2(\frac{1}{\sqrt{x}}), & \text{if } x \geq 1 \\ -\frac{1}{4} \left[\ln \frac{1+\sqrt{1-x}}{1-\sqrt{1-x}} - i\pi \right]^2, & \text{if } x < 1. \end{cases} \tag{28}$$

which originates from the scalar three-point master integral through the relation

$$\mathcal{C}_0(s, 0, 0, m^2, m^2, m^2) = -\frac{2}{s} f\left(\frac{4m^2}{s}\right). \tag{29}$$

2.2 The $\rho\gamma Z$ vertex

The interaction between a dilaton, a photon and a Z boson is described by the $\Gamma_{\gamma Z}^{\alpha\beta}$ correlation function (Figs. 1,2,3). In the on-shell case, with the kinematic defined by

$$p^2 = 0 \quad q^2 = M_Z^2 \quad k^2 = (p+q)^2 = s, \quad (30)$$

the vertex $\Gamma_{\gamma Z}^{\alpha\beta}$ is expanded as

$$\begin{aligned} \Gamma_{\gamma Z}^{\alpha\beta} &= \frac{i}{\Lambda} \left[\mathcal{A}^{\alpha\beta}(p, q) + \Sigma^{\alpha\beta}(p, q) + \Delta^{\alpha\beta}(p, q) \right] \\ &= \frac{i}{\Lambda} \left\{ \left[\frac{1}{2} (s - M_Z^2) \eta^{\alpha\beta} - q^\alpha p^\beta \right] (\mathcal{A}_{\gamma Z} + \Phi_{\gamma Z}(p, q)) + \eta^{\alpha\beta} \Xi_{\gamma Z}(p, q) \right\}. \end{aligned} \quad (31)$$

The anomaly contribution is

$$\mathcal{A}_{\gamma Z} = \frac{\alpha}{\pi s_w c_w} \left[-\frac{1}{3} \sum_f C_v^f Q_f + \frac{1}{12} (37 - 30s_w^2) + 3\chi (c_w^2 - s_w^2) \right], \quad (32)$$

where s_w and c_w to denote the sine and cosine of the θ -Weinberg angle. Here $\Delta^{\alpha\beta}$ is the external leg correction on the dilaton line and the form factors $\Phi(p, q)$ and $\Xi(p, q)$ are introduced to simplify the computation of the decay rate and decomposed as

$$\begin{aligned} \Phi_{\gamma Z}(p, q) &= \Phi_{\gamma Z}^\Sigma(p, q) + \Phi_{\gamma Z}^\Delta(p, q), \\ \Xi_{\gamma Z}(p, q) &= \Xi_{\gamma Z}^\Sigma(p, q) + \Xi_{\gamma Z}^\Delta(p, q), \end{aligned} \quad (33)$$

in order to distinguish the contributions to the external leg corrections (Δ) from those to the cut vertex (Σ). They are given by

$$\begin{aligned} \Phi_{\gamma Z}^\Sigma(p, q) &= \frac{\alpha}{\pi s_w c_w} \left\{ \sum_f C_v^f Q_f \left[\frac{2m_f^2}{s - M_Z^2} + \frac{2m_f^2 M_Z^2}{(s - M_Z^2)^2} \mathcal{D}_0(s, M_Z^2, m_f^2, m_f^2) \right. \right. \\ &\quad \left. \left. - m_f^2 \left(1 - \frac{4m_f^2}{s - M_Z^2} \right) \mathcal{C}_0(s, 0, M_Z^2, m_f^2, m_f^2, m_f^2) \right] - \left[\frac{M_Z^2}{2(s - M_Z^2)} (12s_w^4 - 24s_w^2 + 11) \right. \right. \\ &\quad \left. \left. + \frac{M_Z^2}{2(s - M_Z^2)^2} \left[2M_Z^2 (6s_w^4 - 11s_w^2 + 5) - 2s_w^2 s + s \right] \mathcal{D}_0(s, M_Z^2, M_W^2, M_W^2) \right. \right. \\ &\quad \left. \left. + \frac{M_Z^2 c_w^2}{s - M_Z^2} \left[2M_Z^2 (6s_w^4 - 15s_w^2 + 8) + s(6s_w^2 - 5) \right] \mathcal{C}_0(s, 0, M_Z^2, M_W^2, M_W^2, M_W^2) \right] \right. \\ &\quad \left. \left. + \frac{3\chi(c_w^2 - s_w^2)}{s - M_Z^2} \left[M_Z^2 + s \left(2M_W^2 \mathcal{C}_0(s, 0, M_Z^2, M_W^2, M_W^2, M_W^2) + \frac{M_Z^2}{s - M_Z^2} \mathcal{D}_0(s, M_Z^2, M_W^2, M_W^2) \right) \right] \right\}, \end{aligned}$$

$$\begin{aligned}
\Xi_{\gamma Z}^{\Sigma}(p, q) &= \frac{\alpha}{\pi} \left\{ -\frac{c_w M_Z^2}{s_w} \mathcal{B}_0(0, M_W^2, M_W^2) + 3 s \chi s_w^2 M_Z^2 \mathcal{C}_0(s, 0, M_Z^2, M_W^2, M_W^2, M_W^2) \right\}, \\
\Phi_{\gamma Z}^{\Delta}(p, q) &= \frac{3 \alpha s \chi}{\pi s_w c_w (s - M_H^2)(s - M_Z^2)} \left\{ 2 \sum_f m_f^2 C_v^f Q_f \left[2 + 2 \frac{M_Z^2}{s - M_Z^2} \mathcal{D}_0(s, M_Z^2, m_f^2, m_f^2) \right. \right. \\
&\quad \left. \left. + (4m_f^2 + M_Z^2 - s) \mathcal{C}_0(s, 0, M_Z^2, m_f^2, m_f^2, m_f^2) \right] + M_H^2(1 - 2s_w^2) + 2M_Z^2(6s_w^4 - 11s_w^2 + 5) \right. \\
&\quad \left. + \frac{M_Z^2}{s - M_Z^2} (M_H^2(1 - 2s_w^2) + 2M_Z^2(6s_w^4 - 11s_w^2 + 5)) \mathcal{D}_0(s, M_Z^2, M_W^2, M_W^2) \right. \\
&\quad \left. + 2M_W^2 \mathcal{C}_0(s, 0, M_Z^2, M_W^2, M_W^2, M_W^2) (M_H^2(1 - 2s_w^2) + 2M_Z^2(6s_w^4 - 15s_w^2 + 8) + 2s(4s_w^2 - 3)) \right\} \\
\Xi_{\gamma Z}^{\Delta}(p, q) &= \frac{3 \alpha s \chi c_w}{\pi s_w} M_Z^2 \left\{ \frac{2}{s - M_H^2} \mathcal{B}_0(0, M_W^2, M_W^2) - s_w^2 \mathcal{C}_0(s, 0, M_Z^2, M_W^2, M_W^2, M_W^2) \right\}. \tag{34}
\end{aligned}$$

As for the previous case, we give the decay rate in the simplified limit $\chi \rightarrow 0$ which is easily found to be

$$\begin{aligned}
\Gamma(\rho \rightarrow \gamma Z) &= \frac{9 m_\rho^3}{1024 \Lambda^2 \pi} \sqrt{1 - x_Z} \left(|\Phi_{\gamma Z}^{\Sigma}|^2(p, q) m_\rho^4 (x_Z - 4)^2 + 48 \operatorname{Re} \left\{ \Phi_{\gamma Z}^{\Sigma}(p, q) \Xi_{\gamma Z}^{\Sigma*}(p, q) m_\rho^2 (x_Z - 4) \right\} \right. \\
&\quad \left. - 192 |\Xi_{\gamma Z}^{\Sigma}|^2(p, q) \right), \tag{35}
\end{aligned}$$

where Re is the symbol for the real part.

2.3 The $\rho Z Z$ vertex

The expression for the $\Gamma_{ZZ}^{\alpha\beta}$ vertex (Figs. 1,2,3) defining the $\rho Z Z$ interaction is presented here in the kinematical limit given by $k^2 = (p + q)^2 = s$, $p^2 = q^2 = M_Z^2$ with two on-shell Z bosons. The completely cut correlator takes contributions from a fermion sector, a W gauge boson sector, a $Z - H$ sector together with a term of improvement. There is also an external leg correction $\Delta^{\alpha\beta}$ on the dilaton line which is much more involved than in the previous cases because there are contributions coming from the minimal EMT and from the improved EMT.

At one loop order we have

$$\begin{aligned}
\Gamma_{ZZ}^{\alpha\beta}(p, q) &\equiv \frac{i}{\Lambda} \left[\mathcal{A}^{\alpha\beta}(p, q) + \Sigma^{\alpha\beta}(p, q) + \Delta^{\alpha\beta}(p, q) \right] \\
&= \frac{i}{\Lambda} \left\{ \left[\left(\frac{s}{2} - M_Z^2 \right) \eta^{\alpha\beta} - q^\alpha p^\beta \right] (\mathcal{A}_{ZZ} + \Phi_{ZZ}^{\Sigma}(p, q) + \Phi_{ZZ}^{\Delta}(p, q)) + \eta^{\alpha\beta} (\Xi_{ZZ}^{\Sigma}(p, q) + \Xi_{ZZ}^{\Delta}(p, q)) \right\}, \tag{36}
\end{aligned}$$

where again Σ stands for the completely cut vertex and Δ for the external leg corrections and we have introduced for convenience the separation

$$\begin{aligned}
\Phi_{ZZ}^{\Sigma}(p, q) &= \Phi_{ZZ}^F(p, q) + \Phi_{ZZ}^W(p, q) + \Phi_{ZZ}^{ZH}(p, q) + \Phi_{ZZ}^I(p, q), \\
\Xi_{ZZ}^{\Sigma}(p, q) &= \Xi_{ZZ}^F(p, q) + \Xi_{ZZ}^W(p, q) + \Xi_{ZZ}^{ZH}(p, q) + \Xi_{ZZ}^I(p, q). \tag{37}
\end{aligned}$$

The form factors are given in Appendix F, while here we report only the purely anomalous contribution

$$\mathcal{A}_{ZZ} = \frac{\alpha}{6\pi c_w^2 s_w^2} \left\{ -\sum_f (C_a^{f2} + C_v^{f2}) + \frac{60 s_w^6 - 148 s_w^2 + 81}{4} - \frac{7}{4} + 18 \chi [1 - 2 s_w^2 c_w^2] \right\}. \tag{38}$$

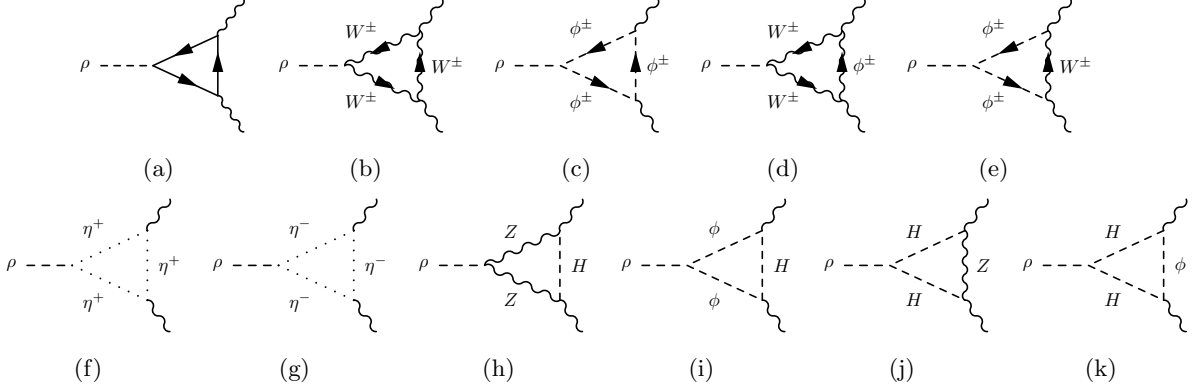


Figure 1: Amplitudes of triangle topology contributing to the $\rho\gamma\gamma$, $\rho\gamma Z$ and ρZZ interactions. They include fermion (F), gauge bosons (B) and contributions from the term of improvement (I). Diagrams (a)-(g) contribute to all the three channels while (h)-(k) only in the ρZZ case.

Finally, we give the decay rate expression for the $\rho \rightarrow ZZ$ process. At leading order it can be computed from the tree level amplitude

$$\mathcal{M}^{\alpha\beta}(\rho \rightarrow ZZ) = \frac{2}{\Lambda} M_Z^2 \eta^{\alpha\beta}, \quad (39)$$

and it is given by

$$\Gamma(\rho \rightarrow ZZ) = \frac{m_\rho^3}{32\pi\Lambda^2} (1-x_Z)^{1/2} \left[1 - x_Z + \frac{3}{4} x_Z^2 \right]. \quad (40)$$

Including the one-loop corrections defined in Eq.(36), one gets the decay rate at next-to-leading order

$$\begin{aligned} \Gamma(\rho \rightarrow ZZ) &= \frac{m_\rho^3}{32\pi\Lambda^2} \sqrt{1-x_Z} \left\{ 1 - x_Z + \frac{3}{4} x_Z^2 + \frac{3}{x_Z} \left[4 \operatorname{Re} \{ \Phi_{ZZ}^\Sigma(p, q) \} (1 - x_Z + \frac{3}{4} x_Z^2) \right. \right. \\ &\quad \left. \left. - \operatorname{Re} \{ \Xi_{ZZ}^\Sigma(p, q) \} m_\rho^2 \left(\frac{3}{4} x_Z^3 - \frac{3}{2} x_Z^2 \right) \right] \right\}. \end{aligned} \quad (41)$$

2.4 Renormalization of dilaton interactions in the broken electroweak phase

In this section we address the renormalization properties of the correlation functions given above. Although the proof is quite cumbersome, one can check, from our previous results, that the 1-loop renormalization of the Standard Model Lagrangian is sufficient to cancel all the singularities in the cut vertices independently of whether the Higgs is conformally coupled or not. Concerning the uncut vertices, instead, the term of improvement plays a significant role in the determination of Green functions which are ultraviolet finite. In particular such a term has to appear with $\chi = 1/6$ in order to guarantee the cancellation of a singularity present in the 1-loop 2-point function describing the Higgs dilaton mixing ($\Sigma_{\rho H}$). The problem arises only in the $\Gamma_{ZZ}^{\alpha\beta}$ correlator, where the $\Sigma_{\rho H}$ two-point function is present as an external leg correction on the dilaton line.

The finite parts of the counterterms are determined in the on-shell renormalization scheme, which is widely used in the electroweak theory. In this scheme the renormalization conditions are fixed in terms of the physical

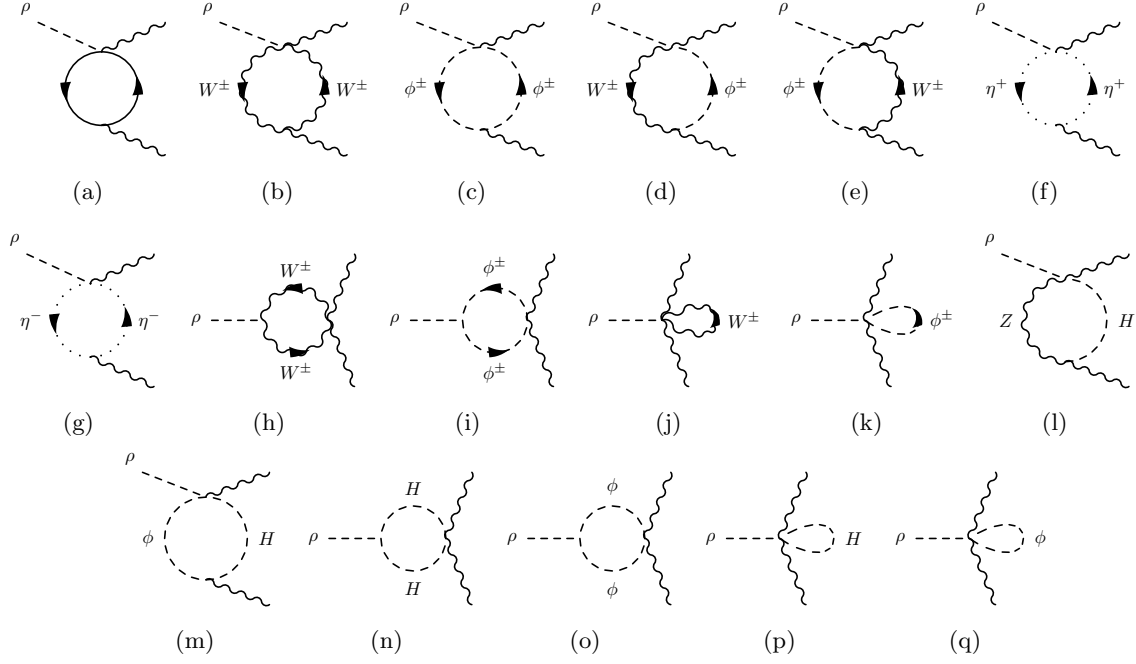


Figure 2: Bubble and tadpole-like diagrams for $\rho\gamma\gamma$, $\rho\gamma Z$ and ρZZ . Amplitudes (l)-(q) contribute only in the ρZZ channel.

parameters to all orders in perturbation theory and the wave-function normalizations of the fields are obtained by requiring a unit residue of the full 2-point functions on the physical particle poles.

From the counterterm Lagrangian we compute the corresponding counterterm to the trace of the EMT. As we have already mentioned, one can also verify from the explicit computation that the terms of improvement, in the conformally coupled case, are necessary to renormalize the vertices containing an intermediate scalar with an external bilinear mixing (dilaton/Higgs). The counterterm vertices for the correlators with a dilaton insertion are

$$\delta[\rho\gamma\gamma]^{\alpha\beta} = 0 \quad (42)$$

$$\delta[\rho\gamma Z]^{\alpha\beta} = -\frac{i}{\Lambda}\delta Z_{Z\gamma} M_Z^2 \eta^{\alpha\beta}, \quad (43)$$

$$\delta[\rho ZZ]^{\alpha\beta} = -2\frac{i}{\Lambda}(M_Z^2 \delta Z_{ZZ} + \delta M_Z^2) \eta^{\alpha\beta}, \quad (44)$$

where the counterterm coefficients are defined in terms of the 2-point functions of the fundamental fields as

$$\delta Z_{Z\gamma} = 2\frac{\Sigma_T^{\gamma Z}(0)}{M_Z^2}, \quad \delta Z_{ZZ} = -\text{Re} \frac{\partial \Sigma_T^{ZZ}(k^2)}{\partial k^2} \Big|_{k^2=M_Z^2}, \quad \delta M_Z^2 = \text{Re} \Sigma_T^{ZZ}(M_Z^2), \quad (45)$$

and are defined in Appendix G. It follows then that the $\rho\gamma\gamma$ interaction must be finite, as one can find by a direct inspection of the $\Gamma_{\gamma\gamma}^{\alpha\beta}$ vertex, while the others require the subtraction of their divergences.

These counterterms are sufficient to remove the divergences of the completely cut graphs which do not contain a bilinear mixing, once we set on-shell the external gauge lines. This occurs both for those diagrams which do not involve the terms of improvement and for those involving T_I . Regarding those contributions which

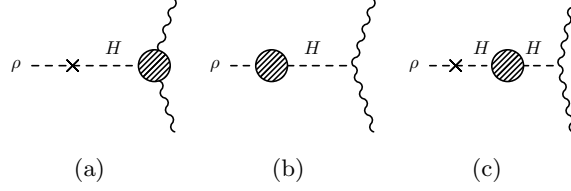


Figure 3: External leg corrections. Diagrams (b) and (c) appear only in the ρZZ sector.

involve the bilinear mixing on the external dilaton line, we encounter two different situations.

In the $\rho\gamma Z$ vertex the insertion of the bilinear mixing ρH generates a reducible diagram of the form Higgs/photon/Z whose renormalization is guaranteed, within the Standard Model, by the use of the Higgs/photon/Z counterterm

$$\delta[H\gamma Z]^{\alpha\beta} = \frac{e M_Z}{2s_w c_w} \delta Z_{Z\gamma} \eta^{\alpha\beta}. \quad (46)$$

As a last case, we discuss the contribution to ρZZ coming from the bilinear mixing, already mentioned above. The corrections on the dilaton line involve the dilaton/Higgs mixing $\Sigma_{\rho H}$, the Higgs self-energy Σ_{HH} and the term of improvement $\Delta_{I, HZZ}^{\alpha\beta}$, which introduces the Higgs/Z/Z vertex (or HZZ) of the Standard Model. The Higgs self-energy and the HZZ vertex, in the Standard Model, are renormalized with the usual counterterms

$$\delta[HH](k^2) = (\delta Z_H k^2 - M_H^2 \delta Z_H - \delta M_H^2), \quad (47)$$

$$\delta[HZZ]^{\alpha\beta} = \frac{e M_Z}{s_w c_w} \left[1 + \delta Z_e + \frac{2s_w^2 - c_w^2}{c_w^2} \frac{\delta s_w}{s_w} + \frac{1}{2} \frac{\delta M_W^2}{M_W^2} + \frac{1}{2} \delta Z_H + \delta Z_{ZZ} \right] \eta^{\alpha\beta}, \quad (48)$$

where

$$\begin{aligned} \delta Z_H &= -Re \frac{\partial \Sigma_{HH}(k^2)}{\partial k^2} \Big|_{k^2=M_H^2}, \quad \delta M_H^2 = Re \Sigma_{HH}(M_H^2), \quad \delta Z_e = -\frac{1}{2} \delta Z_{\gamma\gamma} + \frac{s_w}{2c_w} \delta Z_{Z\gamma}, \\ \delta s_w &= -\frac{c_w^2}{2s_w} \left(\frac{\delta M_W^2}{M_W^2} - \frac{\delta M_Z^2}{M_Z^2} \right), \quad \delta M_W^2 = Re \Sigma_T^{WW}(M_W^2), \quad \delta Z_{\gamma\gamma} = -\frac{\partial \Sigma_T^{\gamma\gamma}(k^2)}{\partial k^2} \Big|_{k^2=0}. \end{aligned} \quad (49)$$

The self-energy $\Sigma_{\rho H}$ is defined by the minimal contribution generated by $T_{Min}^{\mu}{}_{\mu}$ and by a second term derived from $T_I^{\mu}{}_{\mu}$. This second term, with the conformal coupling $\chi = \frac{1}{6}$, is necessary in order to ensure the renormalizability of the dilaton/Higgs mixing. In fact, the use of the minimal EMT in the computation of this self-energy involves a divergence of the form

$$\delta[\rho H]_{Min} = -4 \frac{i}{\Lambda} \delta t, \quad (50)$$

with δt fixed by the condition of cancellation of the Higgs tadpole T_{ad} ($\delta t + T_{ad} = 0$). A simple analysis of the divergences in $\Sigma_{Min, \rho H}$ shows that the counterterm given in Eq. (50) is not sufficient to remove all the singularities of this correlator unless we also include the renormalization constant provided by the term of improvement which is given by

$$\delta[\rho H]_I(k) = -\frac{i}{\Lambda} 6 \chi v \left[\delta v + \frac{1}{2} \delta Z_H \right] k^2, \quad \text{with } \chi = \frac{1}{6}, \quad (51)$$

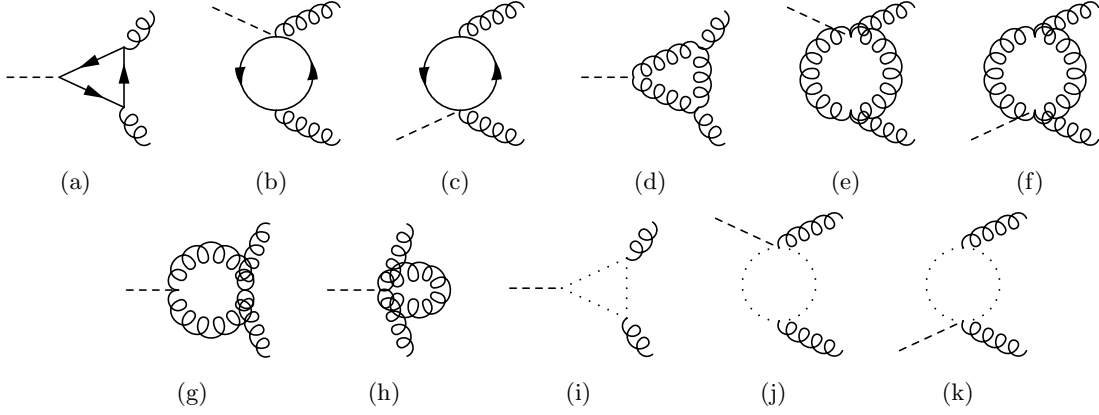


Figure 4: QCD vertices at next-to-leading order. In the on-shell gluon case only diagram (a) contributes.

and

$$\delta v = v \left(\frac{1}{2} \frac{\delta M_W^2}{M_W^2} + \frac{\delta s_w}{s_w} - \delta Z_e \right). \quad (52)$$

One can show explicitly that this counterterm indeed ensures the finiteness of $\Sigma_{\rho H}$.

3 The off-shell dilaton-gluon-gluon vertex in QCD

After a discussion of the leading corrections to the vertices involving one dilaton and two electroweak currents we investigate the interaction of a dilaton and two gluons beyond leading order, giving the expression of the full off-shell vertex. The corresponding interaction with two on-shell gluons has been computed in [2] and is simply given by the contributions of the anomaly and of the quark loop. We will come back to rediscuss the on-shell case in the second part of this work, where we will stress some specific perturbative features of this interaction.

We show in Fig. 4 a list of the NLO QCD contributions to dilaton interactions. As we have just mentioned, in the two-gluon on-shell case one can show by an explicit computation that each of these contributions vanishes, except for diagram (a), which is nonzero when a massive fermion runs in the loop. For this specific reason, in the parton model, the production of the dilaton in pp collisions at the LHC is mediated by the diagram of gluon fusion, which involves a top quark in a loop.

We find convenient to express the result of the off-shell $\Gamma_{gg}^{\alpha\beta}$ vertex in the form

$$\Gamma_{gg}^{\alpha\beta}(p, q) = \frac{i}{\Lambda} \left\{ A^{00}(p, q) \eta^{\alpha\beta} + A^{11}(p, q) p^\alpha p^\beta + A^{22}(p, q) q^\alpha q^\beta + A^{12}(p, q) p^\alpha q^\beta + A^{21}(p, q) q^\alpha p^\beta \right\}, \quad (53)$$

where $A^{ij}(p, q) = A_g^{ij}(p, q) + A_q^{ij}(p, q)$ which are diagonal ($\propto \delta^{ab}$) in color space.

After an explicit computation, we find

$$\begin{aligned} A_g^{00}(p, q) = & -\delta_{ab} \frac{g^2 N_C}{16\pi^2} \left\{ 2 \left(p^2 + q^2 + \frac{11}{3} p \cdot q \right) + (p^2 - q^2) \left[\mathcal{B}_0(p^2, 0, 0) - \mathcal{B}_0(q^2, 0, 0) \right] \right. \\ & \left. + (p^4 + q^4 - 2(p^2 + q^2) p \cdot q - 6p^2 q^2) \mathcal{C}_0((p+q)^2, p^2, q^2, 0, 0, 0) \right\}, \end{aligned}$$

$$A_g^{11}(p, q) = A_g^{22}(q, p) = \delta_{ab} \frac{g^2 N_C}{16 \pi^2} \left\{ 2 + \frac{1}{p \cdot q^2 - p^2 q^2} \left[(p+q)^2 p \cdot q \mathcal{B}_0((p+q)^2, 0, 0) \right. \right. \\ \left. \left. - p^2 (q^2 + p \cdot q) \mathcal{B}_0(p^2, 0, 0) - (2p \cdot q^2 - p^2 q^2 + p \cdot q q^2) \mathcal{B}_0(q^2, 0, 0) \right. \right. \\ \left. \left. + (p^2 q^2 (5q^2 - p^2) + 2p \cdot q^2 (p^2 + p \cdot q - 2q^2)) \mathcal{C}_0((p+q)^2, p^2, q^2, 0, 0, 0) \right] \right\},$$

$$A_g^{12}(p, q) = \delta_{ab} \frac{g^2 N_C}{4 \pi^2} p \cdot q \mathcal{C}_0((p+q)^2, p^2, q^2, 0, 0, 0),$$

$$A_g^{21}(p, q) = \delta_{ab} \frac{g^2 N_C}{24 \pi^2} \left\{ 11 + \frac{3}{2} \frac{1}{p \cdot q^2 - p^2 q^2} (p^2 + q^2) \left[(p^2 + p \cdot q) \mathcal{B}_0(p^2, 0, 0) \right. \right. \\ \left. \left. + (q^2 + p \cdot q) \mathcal{B}_0(q^2, 0, 0) - (p+q)^2 \mathcal{B}_0((p+q)^2, 0, 0) \right. \right. \\ \left. \left. - (p \cdot q (p^2 + 4p \cdot q + q^2) - 2p^2 q^2) \mathcal{C}_0((p+q)^2, p^2, q^2, 0, 0, 0) \right] \right\},$$

$$A_q^{00}(p, q) = \delta_{ab} \frac{g^2}{8 \pi^2} \sum_{i=1}^{n_f} \left\{ \frac{2}{3} p \cdot q - 2m_i^2 + \frac{m_i^2}{p \cdot q^2 - p^2 q^2} \left[p^2 (p \cdot q + q^2) \mathcal{B}_0(p^2, m_i^2, m_i^2) \right. \right. \\ \left. \left. + q^2 (p^2 + p \cdot q) \mathcal{B}_0(q^2, m_i^2, m_i^2) - (p^2 (p \cdot q + 2q^2) + p \cdot q q^2) \mathcal{B}_0((p+q)^2, m_i^2, m_i^2) \right. \right. \\ \left. \left. - (p^2 q^2 (p^2 + q^2 - 4m_i^2) + 4m_i^2 p \cdot q^2 + 4p^2 q^2 p \cdot q - 2p \cdot q^3) \mathcal{C}_0((p+q)^2, p^2, q^2, m_i^2, m_i^2, m_i^2) \right] \right\},$$

$$A_q^{11}(p, q) = A_q^{22}(q, p) = \delta_{ab} \frac{g^2}{8 \pi^2} \sum_{i=1}^{n_f} \frac{2m_i^2 q^2}{p \cdot q^2 - p^2 q^2} \left\{ -2 + \frac{1}{p \cdot q^2 - p^2 q^2} \left[(q^2 (p^2 + 3p \cdot q) \right. \right. \\ \left. \left. + 2p \cdot q^2) \mathcal{B}_0(q^2, m_i^2, m_i^2) + (p^2 (3p \cdot q + q^2) + 2p \cdot q^2) \mathcal{B}_0(p^2, m_i^2, m_i^2) \right. \right. \\ \left. \left. - (p^2 (3p \cdot q + 2q^2) + p \cdot q (4p \cdot q + 3q^2)) \mathcal{B}_0((p+q)^2, m_i^2, m_i^2) \right. \right. \\ \left. \left. - (2p \cdot q^2 (2m_i^2 + p^2 + q^2) + p^2 q^2 (p^2 + q^2 - 4m_i^2)) \right. \right. \\ \left. \left. + 4p^2 q^2 p \cdot q + 2p \cdot q^3) \mathcal{C}_0((p+q)^2, p^2, q^2, m_i^2, m_i^2, m_i^2) \right] \right\},$$

$$A_q^{12}(p, q) = \delta_{ab} \frac{g^2}{8 \pi^2} \sum_{i=1}^{n_f} \frac{2m_i^2 p \cdot q^2}{p \cdot q^2 - p^2 q^2} \left\{ 2 + \frac{1}{p \cdot q^2 - p^2 q^2} \left[- (q^2 (p^2 + 3p \cdot q) + 2p \cdot q^2) \mathcal{B}_0(q^2, m_i^2, m_i^2) \right. \right. \\ \left. \left. - (p^2 (3p \cdot q + q^2) + 2p \cdot q^2) \mathcal{B}_0(p^2, m_i^2, m_i^2) + (p^2 (3p \cdot q + 2q^2) + p \cdot q (4p \cdot q + 3q^2)) \right. \right. \\ \times \mathcal{B}_0((p+q)^2, m_i^2, m_i^2) + (2p \cdot q^2 (2m_i^2 + p^2 + q^2) + p^2 q^2 (p^2 + q^2 - 4m_i^2)) \\ \left. \left. + 4p^2 q^2 p \cdot q + 2p \cdot q^3) \mathcal{C}_0((p+q)^2, p^2, q^2, m_i^2, m_i^2, m_i^2) \right] \right\},$$

$$A_q^{21}(p, q) = \delta_{ab} \frac{g^2}{8 \pi^2} \sum_{i=1}^{n_f} \left\{ -\frac{2}{3} + \frac{2m_i^2 p \cdot q}{p \cdot q - p^2 q^2} + \frac{m_i^2}{(p \cdot q - p^2 q^2)^2} \left[-p^2 (q^2 (2p^2 + 3p \cdot q) + p \cdot q^2) \right. \right. \\ \times \mathcal{B}_0(p^2, m_i^2, m_i^2) - q^2 (p^2 (3p \cdot q + 2q^2) + p \cdot q^2) \mathcal{B}_0(q^2, m_i^2, m_i^2) + (2p^4 q^2 + p^2 (6p \cdot q q^2 \\ + p \cdot q^2 + 2q^4) + p \cdot q^2 q^2) \mathcal{B}_0((p+q)^2, m_i^2, m_i^2) + p \cdot q (p^2 q^2 (3p^2 + 3q^2 - 4m_i^2) \\ \left. \left. + 4m_i^2 p \cdot q^2 + 8p^2 q^2 p \cdot q - 2p \cdot q^3) \mathcal{C}_0((p+q)^2, p^2, q^2, m_i^2, m_i^2, m_i^2) \right] \right\}, \quad (54)$$

where N_C is the number of colors, n_f is the number of flavor and m_i the mass of the quark. In the on-shell gluon case, Eq.(53) reproduces the same interaction responsible for Higgs production at LHC augmented by an anomaly term. This is given by

$$\Gamma_{gg}^{\alpha\beta}(p, q) = \frac{i}{\Lambda} \Phi(s) u^{\alpha\beta}(p, q), \quad (55)$$

with $u^{\alpha\beta}(p, q)$ defined in Eq.(21), and with the gluon/quark contributions included in the $\Phi(s)$ form factor ($s = k^2 = (p + q)^2$)

$$\Phi(s) = -\delta^{ab} \frac{g^2}{24\pi^2} \left\{ (11 N_C - 2 n_f) + 12 \sum_{i=1}^{n_f} m_i^2 \left[\frac{1}{s} - \frac{1}{2} \mathcal{C}_0(s, 0, 0, m_i^2, m_i^2, m_i^2) \left(1 - \frac{4m_i^2}{s} \right) \right] \right\}, \quad (56)$$

where the first mass independent terms represent the contribution of the anomaly, while the others are the explicit mass corrections.

The decay rate of a dilaton in two gluons can be evaluated from the on-shell limit in Eq.(55) and it is given by

$$\Gamma(\rho \rightarrow gg) = \frac{\alpha_s^2 m_\rho^3}{32 \pi^3 \Lambda^2} \left| \beta_{QCD} + x_t [1 + (1 - x_t) f(x_t)] \right|^2, \quad (57)$$

where we have taken the top quark as the only massive fermion and x_i and $f(x_i)$ are defined in Eq. (27) and Eq. (28) respectively. Moreover we have set $\beta_{QCD} = 11N_C/3 - 2n_f/3$ for the QCD β function.

4 Non-gravitational dilatons from scale-invariant extensions of the Standard Model

As we have pointed out in the introduction, a dilaton may appear in the spectrum of different extensions of the Standard Model not only as a result of the compactification of extra spacetime dimensions, but also as an effective state, related to the breaking of a dilatation symmetry. In this respect, notice that in its actual formulation the Standard Model is not scale-invariant, but can be such, at classical level, if we slightly modify the scalar potential with the introduction of a dynamical field Σ that allows to restore this symmetry and acquires a vacuum expectation value. This task is accomplished by the replacement of every dimensionfull parameter m according to $m \rightarrow m \frac{\Sigma}{\Lambda}$, where Λ is the classical conformal breaking scale. In the case of the Standard Model, classical scale invariance can be easily accomodated with a simple change of the scalar potential.

This is defined, obviously, modulo a constant, therefore we may consider, for instance, two equivalent choices

$$\begin{aligned} V_1(H, H^\dagger) &= -\mu^2 H^\dagger H + \lambda (H^\dagger H)^2 = \lambda \left(H^\dagger H - \frac{\mu^2}{2\lambda} \right)^2 - \frac{\mu^4}{4\lambda} \\ V_2(H, H^\dagger) &= \lambda \left(H^\dagger H - \frac{\mu^2}{2\lambda} \right)^2 \end{aligned} \quad (58)$$

which gives two *different* scale-invariant extensions

$$\begin{aligned} V_1(H, H^\dagger, \Sigma) &= -\frac{\mu^2 \Sigma^2}{\Lambda^2} H^\dagger H + \lambda (H^\dagger H)^2 \\ V_2(H, H^\dagger, \Sigma) &= \lambda \left(H^\dagger H - \frac{\mu^2 \Sigma^2}{2\lambda \Lambda^2} \right)^2, \end{aligned} \quad (59)$$

where H is the Higgs doublet, λ is its dimensionless coupling constant, while μ has the dimension of a mass and, therefore, is the only term involved in the scale invariant extension. More details of this analysis can be found in appendix B.

The invariance of the potential under the addition of constant terms, typical of any Lagrangian, is lifted once we require the presence of a dilatation symmetry. Only the second choice (V_2) guarantees the existence of a stable ground state characterized by a spontaneously broken phase. In V_2 we parameterize the Higgs, as usual, around the electroweak vev v as in Eq.(12), and indicate with Λ the vev of the dilaton field $\Sigma = \Lambda + \rho$, and we have set $\phi^+ = \phi = 0$ in the unitary gauge.

The potential V_2 has a massless mode due to the existence of a flat direction. Performing a diagonalization of the mass matrix we define the two mass eigenstates ρ_0 and h_0 , which are given by

$$\begin{pmatrix} \rho_0 \\ h_0 \end{pmatrix} = \begin{pmatrix} \cos \alpha & \sin \alpha \\ -\sin \alpha & \cos \alpha \end{pmatrix} \begin{pmatrix} \rho \\ h \end{pmatrix} \quad (60)$$

with

$$\cos \alpha = \frac{1}{\sqrt{1 + v^2/\Lambda^2}} \quad \sin \alpha = \frac{1}{\sqrt{1 + \Lambda^2/v^2}}. \quad (61)$$

We denote with ρ_0 the massless dilaton generated by this potential, while h_0 will describe a massive scalar, interpreted as a new Higgs field, whose mass is given by

$$m_{h_0}^2 = 2\lambda v^2 \left(1 + \frac{v^2}{\Lambda^2}\right) \quad \text{with} \quad v^2 = \frac{\mu^2}{\lambda}, \quad (62)$$

and with $m_h^2 = 2\lambda v^2$ being the mass of the Standard Model Higgs. The Higgs mass, in this case, is corrected by the new scale of the spontaneous breaking of the dilatation symmetry (Λ), which remains a free parameter.

The vacuum degeneracy of the scale-invariant model can be lifted by the introduction of extra (explicit breaking) terms which give a small mass to the dilaton field. To remove such degeneracy, one can introduce, for instance, the term

$$\mathcal{L}_{break} = \frac{1}{2} m_\rho^2 \rho^2 + \frac{1}{3!} m_\rho^2 \frac{\rho^3}{\Lambda} + \dots, \quad (63)$$

where m_ρ represents the dilaton mass.

It is clear that in this approach the coupling of the dilaton to the anomaly has to be added by hand. The obvious question to address, at this point, is if one can identify in the effective action of the Standard Model an effective state which may interpolate between the dilatation current of the same model and the final state with two neutral currents, for example with two photons. The role of the following sections will be to show rigorously that such a state can be identified in ordinary perturbation theory in the form of an anomaly pole.

We will interpret this scalar exchange as a composite state whose interactions with the rest of the Standard Model are defined by the conditions of scale and gauge invariance. In this respect, the Standard Model Lagrangian, enlarged by the introduction of a potential of the form $V_2(H, H^\dagger, \Sigma)$, which is expected to capture the dynamics of this pseudo-Goldstone mode, could take the role of a workable model useful for a phenomenological analysis. We will show rigorously that this state couples to the conformal anomaly by a direct analysis of the $J_D V V$ correlator, in the form of an anomaly pole, with J_D and V being the dilatation and a vector current respectively. Usual polology arguments support the fact that a pole in a correlation function is there to indicate

that a specific state can be created by a field operator in the Lagrangian of the theory, or, alternatively, as a composite particle of the same elementary fields.

Obviously, a perturbative hint of the existence of such intermediate state does not correspond to a complete description of the state, in the same way as the discovery of an anomaly pole in the AVV correlator of QCD (with A being the axial current) is not equivalent to a proof of the existence of the pion. Nevertheless, massless poles extracted from the perturbative effective action do not appear for no reasons, and their infrared couplings should trigger further phenomenological interest.

4.1 The $J_D VV$ and TVV vertices

This effective degree of freedom emerges both from the spectral analysis of the TVV [4, 5] and, as we are now going to show, of the $J_D VV$ vertices, being the two vertices closely related. We recall that the dilatation current can be defined as

$$J_D^\mu(z) = z_\nu T^{\mu\nu}(z) \quad \text{with} \quad \partial \cdot J_D = T^\mu{}_\mu. \quad (64)$$

The $T^{\mu\nu}$ has to be symmetric and on-shell traceless for a classical scale-invariant theory, and includes, at quantum level, the contribution from the trace anomaly together with the additional terms describing the explicit breaking of the dilatation symmetry. The separation between the anomalous and the explicit contributions to the breaking of dilatation symmetry is present in all the analysis that we have performed on the TVV vertex in dimensional regularization. In this respect, the analogy between these types of correlators and the AVV diagram of the chiral anomaly goes quite far, since in the AVV case such a separation has been shown to hold in the Longitudinal/Transverse (L/T) solution of the anomalous Ward identities [6, 7, 8]. This has been verified in perturbation theory in the same scheme.

We recall that the $U(1)_A$ current is characterized by an anomaly pole which describes the interaction between the Nambu-Goldstone mode, generated by the breaking of the chiral symmetry, and the gauge currents. In momentum space this corresponds to the nonlocal vertex

$$V_{\text{anom}}^{\lambda\mu\nu}(k, p, q) = \frac{k^\lambda}{k^2} \epsilon^{\mu\nu\alpha\beta} p_\alpha q_\beta + \dots \quad (65)$$

with k being the momentum of the axial-vector current and p and q the momenta of the two photons. In the equation above, the ellipsis refer to terms which are suppressed at large energy. In this regime, this allows to distinguish the operator accounting for the chiral anomaly (i.e. \Box^{-1} in coordinate space) from the contributions due to mass corrections. Polology arguments can be used to relate the appearance of such a pole to the pion state around the scale of chiral symmetry breaking.

To identify the corresponding pole in the dilatation current of the $J_D VV$ correlator at zero momentum transfer, one can follow the analysis of [9], where it is shown that the appearance of the trace anomaly is related to the presence of a superconvergent sum rule in the spectral density of this correlator. At nonzero momentum transfer the derivation of a similar behaviour can be obtained by an explicit computation of the spectral density of the TVV vertex [4] or of the entire correlator, as done for QED and QCD [5, 10] and as we will show next.

Using the relation between J_D^μ and the EMT $T^{\mu\nu}$ we introduce the $J_D VV$ correlator

$$\Gamma_D^{\mu\alpha\beta}(k, p) \equiv \int d^4z d^4x e^{-ik \cdot z + ip \cdot x} \left\langle J_D^\mu(z) V^\alpha(x) V^\beta(0) \right\rangle \quad (66)$$

which can be related to the TVV correlator

$$\Gamma^{\mu\nu\alpha\beta}(k, p) \equiv \int d^4z d^4x e^{-ik \cdot z + ip \cdot x} \langle T^{\mu\nu}(z) V^\alpha(x) V^\beta(0) \rangle \quad (67)$$

according to

$$\Gamma_D^{\mu\alpha\beta}(k, p) = i \frac{\partial}{\partial k^\nu} \Gamma^{\mu\nu\alpha\beta}(k, p). \quad (68)$$

As we have already mentioned, this equation allows us to identify a pole term in the $J_D VV$ diagram from the corresponding pole structure in the TVV vertex. In the following we will show the emergence of the anomaly poles in the QED and QCD cases.

4.2 The dilaton anomaly pole in the QED case

For definiteness, it is convenient to briefly review the characterization of the TVV vertex in the QED case with a massive fermion (see [5] for more details). The full amplitude can be expanded in a specific basis of 13 tensors first identified in [4]

$$\Gamma^{\mu\nu\alpha\beta}(p, q) = \sum_{i=1}^{13} F_i(s; s_1, s_2, m^2) \phi_i^{\mu\nu\alpha\beta}(p, q), \quad (69)$$

where the 13 invariant amplitudes F_i are functions of the kinematical invariants $s = k^2 = (p + q)^2$, $s_1 = p^2$, $s_2 = q^2$, with p and q the momenta of the external photons, and of the internal fermion mass m . The list of the tensor structures ϕ_i can be found in [4]. The number of these form factors reduces from 13 to 3 in the case of on-shell photons. For our purposes, being interested in the appearance of the anomaly poles, we only need the contributions that generate a non zero trace. These come from the tensors $\phi_1^{\mu\nu\alpha\beta}$ and $\phi_2^{\mu\nu\alpha\beta}$ which are

$$\begin{aligned} \phi_1^{\mu\nu\alpha\beta} &= (k^2 \eta^{\mu\nu} - k^\mu k^\nu) u^{\alpha\beta}(p, q), \\ \phi_2^{\mu\nu\alpha\beta} &= (k^2 \eta^{\mu\nu} - k^\mu k^\nu) w^{\alpha\beta}(p, q), \end{aligned} \quad (70)$$

where

$$\begin{aligned} u^{\alpha\beta}(p, q) &\equiv (p \cdot q) \eta^{\alpha\beta} - q^\alpha p^\beta, \\ w^{\alpha\beta}(p, q) &\equiv p^2 q^2 \eta^{\alpha\beta} + (p \cdot q) p^\alpha q^\beta - q^2 p^\alpha p^\beta - p^2 q^\alpha q^\beta. \end{aligned} \quad (71)$$

For two on-shell final state photons ($s_1 = s_2 = 0$) and a massive fermion we obtain

$$F_1(s; 0, 0, m^2) = F_{1pole} + \frac{e^2 m^2}{3 \pi^2 s^2} - \frac{e^2 m^2}{3 \pi^2 s} \mathcal{C}_0(s, 0, 0, m^2, m^2, m^2) \left[\frac{1}{2} - \frac{2m^2}{s} \right], \quad (72)$$

where

$$F_{1pole} = -\frac{e^2}{18 \pi^2 s} \quad (73)$$

and the scalar three-point function $\mathcal{C}_0(s, 0, 0, m^2, m^2, m^2)$ is given by

$$\mathcal{C}_0(s, 0, 0, m^2, m^2, m^2) = \frac{1}{2s} \log^2 \frac{a_3 + 1}{a_3 - 1}, \quad \text{with } a_3 = \sqrt{1 - 4m^2/s}. \quad (74)$$

In the massless fermion case two properties of this expansion are noteworthy: 1) the trace anomaly takes contribution only from a single tensor structure (ϕ_1) and invariant amplitude (F_1) which coincides with the pole term; 2) the residue of this pole as $s \rightarrow 0$ is nonzero, showing that the pole is coupled in the infrared. Notice that the form factor F_2 , which in general gives a nonzero contribution to the trace in the presence of mass terms, is multiplied by a tensor structure (ϕ_2) which *vanishes* when the two photons are on-shell. Therefore, similarly to the case of the chiral anomaly, also in this case the anomaly is *entirely* given by the appearance of an anomaly pole. We stress that this result is found to be exact in dimensional regularization, which is a mass independent scheme: at perturbative level, the anomalous breaking of the dilatation symmetry, related to an anomaly pole in the spectrum of all the gauge-invariant correlators studied in this work, is separated from the sources of *explicit* breaking. The latter are related to the mass parameters and/or to the gauge bosons virtualities p^2 and q^2 .

To analyze the implications of the pole behaviour discussed so far for the TVV vertex and its connection with the $J_D VV$ correlator, we limit our attention on the anomalous contribution ($F_1 \phi_1^{\mu\nu\alpha\beta}$), which we rewrite in the form

$$\Gamma_{pole}^{\mu\nu\alpha\beta}(k, p) \equiv -\frac{e^2}{18\pi^2} \frac{1}{k^2} (\eta^{\mu\nu} k^2 - k^\mu k^\nu) u^{\alpha\beta}(p, q), \quad q = k - p. \quad (75)$$

This implies that the $J_D VV$ correlator acquires a pole as well

$$\Gamma_{Dpole}^{\mu\alpha\beta} = -i \frac{e^2}{18\pi^2} \frac{\partial}{\partial k^\nu} \left[\frac{1}{k^2} (\eta^{\mu\nu} k^2 - k^\mu k^\nu) u^{\alpha\beta}(p, k - p) \right] \quad (76)$$

and acting with the derivative on the right hand side we finally obtain

$$\Gamma_{Dpole}^{\mu\alpha\beta}(k, p) = i \frac{e^2}{6\pi^2} \frac{k^\mu}{k^2} u^{\alpha\beta}(p, k - p) - i \frac{e^2}{18\pi^2} \frac{1}{k^2} (\eta^{\mu\nu} k^2 - k^\mu k^\nu) \frac{\partial}{\partial k_\nu} u^{\alpha\beta}(p, k - p). \quad (77)$$

Notice that the first contribution on the right hand side of the previous equation corresponds to an anomaly pole, shown pictorially in Fig. 5. In fact, by taking a derivative of the dilatation current only this term will contribute to the corresponding Ward identity

$$k_\mu \Gamma_D^{\mu\alpha\beta}(k, p) = i \frac{e^2}{6\pi^2} u^{\alpha\beta}(p, k - p), \quad (78)$$

which is the expression in momentum space of the usual relation $\partial J_D \sim FF$, while the second term trivially vanishes. Notice that the pole in (78) has disappeared, and we are left just with its residue on the r.h.s., or, equivalently, the pole is removed in Eq. (75) if we trace the two indices (μ, ν).

4.3 The dilaton anomaly pole in the QCD case

The analysis presented for the dilatation current of QED can be immediately generalized to the case of QCD. Following a similar reasoning, we expand the on-shell TVV vertex, with V denoting now the gluon, as

$$\Gamma^{\mu\nu\alpha\beta}(p, q) = \delta^{ab} \sum_{i=1}^3 \Phi_i(s; 0, 0) t_i^{\mu\nu\alpha\beta}(p, q) \quad \text{with} \quad p^2 = q^2 = 0, \quad (79)$$

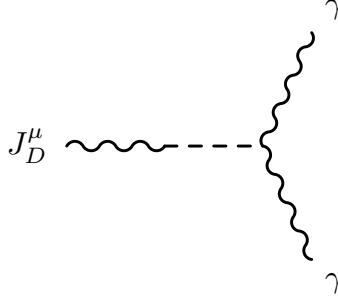


Figure 5: Exchange of a dilaton pole mediated by the $J_D V V$ correlator.

with the tensor basis given by

$$\begin{aligned}
t_1^{\mu\nu\alpha\beta}(p, q) &= (s \eta^{\mu\nu} - k^\mu k^\nu) u^{\alpha\beta}(p, q), \\
t_2^{\mu\nu\alpha\beta}(p, q) &= -2 u^{\alpha\beta}(p, q) [s \eta^{\mu\nu} + 2(p^\mu p^\nu + q^\mu q^\nu) - 4(p^\mu q^\nu + q^\mu p^\nu)], \\
t_3^{\mu\nu\alpha\beta}(p, q) &= (p^\mu q^\nu + p^\nu q^\mu) g^{\alpha\beta} + \frac{s}{2} (\eta^{\alpha\nu} \eta^{\beta\mu} + \eta^{\alpha\mu} \eta^{\beta\nu}) \\
&\quad - \eta^{\mu\nu} \left(\frac{s}{2} \eta^{\alpha\beta} - q^\alpha p^\beta \right) - (\eta^{\beta\nu} p^\mu + \eta^{\beta\mu} p^\nu) q^\alpha - (\eta^{\alpha\nu} q^\mu + \eta^{\alpha\mu} q^\nu) p^\beta,
\end{aligned} \tag{80}$$

where δ^{ab} is the diagonal matrix in color space. Again we have $s = k^2 = (p + q)^2$, with the virtualities of the two gluons being $p^2 = q^2 = 0$. Notice that in the massless fermion limit only the first (t_1) of these 3 form factors contributes to the anomaly. The corresponding on-shell form factors with massive quarks are

$$\begin{aligned}
\Phi_1(s; 0, 0) &= -\frac{g^2}{72\pi^2 s} (2n_f - 11N_C) + \frac{g^2}{6\pi^2} \sum_{i=1}^{n_f} m_i^2 \left\{ \frac{1}{s^2} - \frac{1}{2s} \mathcal{C}_0(s, 0, 0, m_i^2, m_i^2, m_i^2) \left[1 - \frac{4m_i^2}{s} \right] \right\}, \\
\Phi_2(s; 0, 0) &= -\frac{g^2}{288\pi^2 s} (n_f - N_C) \\
&\quad - \frac{g^2}{24\pi^2} \sum_{i=1}^{n_f} m_i^2 \left\{ \frac{1}{s^2} + \frac{3}{s^2} \mathcal{D}_0(s, 0, 0, m_i^2, m_i^2) + \frac{1}{s} \mathcal{C}_0(s, 0, 0, m_i^2, m_i^2, m_i^2) \left[1 + \frac{2m_i^2}{s} \right] \right\}, \\
\Phi_3(s; 0, 0) &= \frac{g^2}{288\pi^2} (11n_f - 65N_C) - \frac{g^2 N_C}{8\pi^2} \left[\frac{11}{6} \mathcal{B}_0(s, 0, 0) - \mathcal{B}_0(0, 0, 0) + s \mathcal{C}_0(s, 0, 0, 0, 0, 0) \right] \\
&\quad + \frac{g^2}{8\pi^2} \sum_{i=1}^{n_f} \left\{ \frac{1}{3} \mathcal{B}_0(s, m_i^2, m_i^2) + m_i^2 \left[\frac{1}{s} + \frac{5}{3s} \mathcal{D}_0(s, 0, 0, m_i^2) + \mathcal{C}_0(s, 0, 0, m_i^2, m_i^2, m_i^2) \left[1 + \frac{2m_i^2}{s} \right] \right] \right\},
\end{aligned} \tag{81}$$

where m_i denotes the quark mass, and we have summed over the fermion flavours (n_f), while N_C denotes the number of colors. Notice the appearance of the $1/s$ pole in Φ_1 , which saturates the contribution to the trace anomaly in the massless limit which becomes

$$\Phi_1(s; 0, 0) = -\frac{g^2}{72\pi^2 s} (2n_f - 11N_C). \tag{82}$$

As for the QED case, this is the only invariant amplitude which contributes to the anomalous trace part of the correlator. The pole completely accounts for the trace anomaly and is clearly inherited by the QCD dilatation

current, for the same reasonings discussed above.

4.4 Mass corrections to the dilaton pole

The discussion of the mass corrections to the massless dilaton can follow quite closely the strategy adopted in the pion case using partially conserved axial currents (PCAC) techniques. Also in this case, as for PCAC in the past, one can assume a partially conserved dilaton current (PCDC) in order to relate the decay amplitude of the dilaton f_ρ to its mass m_ρ and to the vacuum energy.

For this goal we define the 1-particle transition amplitudes for the dilatation current and the EMT between the vacuum and a dilaton state with momentum p_μ

$$\begin{aligned}\langle 0|J_D^\mu(x)|\rho, p\rangle &= -i f_\rho p^\mu e^{-ip \cdot x} \\ \langle 0|T^{\mu\nu}(x)|\rho, p\rangle &= \frac{f_\rho}{3} (p^\mu p^\nu - \eta^{\mu\nu} p^2) e^{-ip \cdot x},\end{aligned}\tag{83}$$

both of them giving

$$\partial_\mu \langle 0|J_D^\mu(x)|\rho, p\rangle = \eta_{\mu\nu} \langle 0|T^{\mu\nu}(x)|\rho, p\rangle = -f_\rho m_\rho^2 e^{-ip \cdot x}.\tag{84}$$

We introduce the dilaton interpolating field $\rho(x)$ via a PCDC relation

$$\partial_\mu J_D^\mu(x) = -f_\rho m_\rho^2 \rho(x)\tag{85}$$

with

$$\langle 0|\rho(x)|\rho, p\rangle = e^{-ip \cdot x}\tag{86}$$

and the matrix element

$$\mathcal{A}^\mu(q) = \int d^4x e^{iq \cdot x} \langle 0|T\{J_D^\mu(x)T^\alpha_\alpha(0)\}|0\rangle,\tag{87}$$

where $T\{\dots\}$ denotes the time ordered product.

Using dilaton pole dominance we can rewrite the contraction of q_μ with this correlator as

$$\lim_{q_\mu \rightarrow 0} q_\mu \mathcal{A}^\mu(q) = f_\rho \langle \rho, q=0|T^\alpha_\alpha(0)|0\rangle,\tag{88}$$

where the soft limit $q_\mu \rightarrow 0$ with $q^2 \gg m_\rho^2 \sim 0$ has been taken.

At the same time the dilatation Ward identity on the amplitude $\mathcal{A}^\mu(q)$ in Eq.(87) gives

$$\begin{aligned}q_\mu \mathcal{A}^\mu(q) &= i \int d^4x e^{iq \cdot x} \frac{\partial}{\partial x^\mu} \langle 0|T\{J_D^\mu(x)T^\alpha_\alpha(0)\}|0\rangle \\ &= i \int d^4x e^{iq \cdot x} \langle 0|T\{\partial_\mu J_D^\mu(x)T^\alpha_\alpha(0)\}|0\rangle + i \int d^4x e^{iq \cdot x} \delta(x_0) \langle 0|[J_D^0(x), T^\alpha_\alpha(0)]|0\rangle.\end{aligned}\tag{89}$$

The commutator of the time component of the dilatation charge density and the trace of the EMT can be rewritten as

$$[J_D^0(0, \mathbf{x}), T^\alpha_\alpha(0)] = -i\delta^3(\mathbf{x}) (d_T + x \cdot \partial) T^\alpha_\alpha(0)\tag{90}$$

where d_T is the canonical dimension of the EMT ($d_T = 4$). Inserting Eq.(90) in the Ward identity (89) and neglecting the first term due to the nearly conserved dilatation current ($m_\rho \sim 0$), we are left with

$$q_\mu \mathcal{A}^\mu(q) = d_T \langle 0|T^\alpha_\alpha(0)|0\rangle.\tag{91}$$

In the soft limit, with $q^2 \gg m_\rho^2$, comparing Eq.(88) and Eq.(91) we obtain

$$\lim_{q^\mu \rightarrow 0} q^\mu \mathcal{A}_\mu = f_\rho \langle \rho, q = 0 | T^\alpha_\alpha(0) | 0 \rangle = d_T \langle 0 | T^\alpha_\alpha(0) | 0 \rangle. \quad (92)$$

Introducing the vacuum energy density $\epsilon_{vac} = \langle 0 | T^0_0 | 0 \rangle = \frac{1}{4} \langle 0 | T^\alpha_\alpha(0) | 0 \rangle$ and using the relation in Eq.(84) we have

$$\langle \rho, p = 0 | T^\mu_\mu | 0 \rangle = -f_\rho m_\rho^2 = \frac{d_T}{f_\rho} \epsilon_{vac} \quad (93)$$

from which we finally obtain ($d_T = 4$)

$$f_\rho^2 m_\rho^2 = -16 \epsilon_{vac}. \quad (94)$$

This equation fixes the decay amplitude of the dilaton in terms of its mass and the vacuum energy. Notice that ϵ_{vac} can be related both to the anomaly and possibly to explicit contributions of the breaking of the dilatation symmetry since

$$\epsilon_{vac} = \frac{1}{4} \left\langle 0 \left| \frac{\beta(g)}{2g} F_{\mu\nu} F^{\mu\nu} \right| 0 \right\rangle + \dots \quad (95)$$

where the ellipsis saturate the anomaly equation with extra mass-dependent contributions, which may be far larger in size than the anomaly term. In (95) we have assumed, for simplicity, the coupling of the pole to a single gauge field, with a beta function $\beta(g)$, but obviously, it can be generalized to several gauge fields.

In the case of higher dimensional operators we would get

$$\epsilon_{vac} = \frac{1}{4} \left\langle 0 \left| \frac{\beta(g)}{2g} F_{\mu\nu} F^{\mu\nu} \right| 0 \right\rangle + \sum_i g_i (d_i - 4) \langle 0 | O_i | 0 \rangle, \quad (96)$$

valid around the scale at which the PCDC approximation holds. Therefore a massless pole can be corrected nonperturbatively according to some completion theory, causing its mass to shift. Perturbation theory gives indications about the interpolating fields which can couple to it, as we have seen by exploiting the chiral analogy, but not more than that. The corrections are model-dependent and can be the subject of additional phenomenological searches, but the dilatation current takes the role, with no doubt, of an interpolating field for the propagation of such a scalar intermediate state.

5 The infrared coupling of an anomaly pole and the anomaly enhancement

It is easy to figure out from the results of the previous sections that the coupling of a (graviscalar) dilaton to the anomaly causes a large enhancement of its 2-photons and 2-gluons decays. One of the features of the graviscalar interaction is that its coupling includes anomalous contributions which are part both of the two-photon and of the two-gluon cross sections. For this reason, if an enhancement respect to the Standard Model rates is found only in one of these two channels and it is associated to the exchange of a spin zero intermediate state, this result could be used to rule out the exchange of a graviscalar.

On the other hand, for an effective dilaton, identified by an anomaly pole in the $J_D VV$ correlator of the Standard Model, the case is more subtle, since the coupling of this effective state to the anomaly has to be introduced by hand. This state should be identified, in the perturbative picture, with the corresponding anomaly

pole. The situation, here, is closely similar to the pion case, where the anomalous contribution to the pion-photon-photon vertex is added - a posteriori - to a Lagrangian which is otherwise chirally symmetric. Also in the pion case the anomaly enhancement can be justified, in a perturbative approach, by the infrared coupling of the anomaly pole of the AVV diagram.

In general, in the case of an effective dilaton, one is allowed to write down a Lagrangian which is assumed to be scale invariant and, at a second stage, introduce the direct coupling of this state to the trace anomaly. The possibility of coupling such a state to the photon and to the gluons or just to the photons, for instance, is a delicate issue for which a simple perturbative approach is unable to offer a definitive answer. For instance, if we insist that confinement does not allow us to have, in any case, on-shell final state gluons, the two-gluon coupling of an effective dilaton, identified in the corresponding $J_D VV$ correlator, should not be anomaly enhanced. In fact, with one or two off-shell final state gluons, the residue of the anomaly pole in this correlator is zero. Few more comments on this issue can be found in appendix A.

We feel, however, that a simple perturbative analysis may not be completely sufficient to decide whether or not the coupling of such a state to the gluon anomaly takes place. On the other hand, there is no doubt, by the same reason, that such a coupling should occur in the 2-photon case, being the photons massless asymptotic states. In this case the corresponding anomaly pole of the $J_D \gamma\gamma$ vertex is infrared coupled.

Similar enhancements are present in the case of quantum scale invariant extensions of the Standard Model [11], where one assumes that the spectrum of the theory is extended with new massive states in order to set the β functions of the gauge couplings to vanish. In a quantum scale invariant theory such as the one discussed in [11], the dilaton couples only to massive states, but the heavy mass limit and the condition of the vanishing of the complete β functions, leave at low energy a dilaton interaction proportional only to the β functions of the low energy states. We have commented on this point in appendix C. The "remnant" low energy interaction is mass-independent and coincides with that due to a typical anomalous coupling, although its origin is of different nature, since anomalous contributions are genuinely mass-independent.

For this reason, the decays of a dilaton produced by such extensions carries "anomaly like" enhancements as in the graviscalar case. Obviously, such enhancements to the low energy states of the Standard Model would also be typical of the decay of a Higgs field, which couples proportionally to the mass of an intermediate state, if quantum scale invariance is combined with the decoupling of a heavy sector. This, in general, causes an enhancement of the Higgs decay rates into photons and gluons. A partial enhancement only of the di-photon channel could be accomplished, in this approach, by limiting the above quantum scale invariant arguments only to the electroweak sector.

6 Conclusions

We have presented a general discussion of dilaton interactions with the neutral currents sector of the Standard Model. In the case of a fundamental graviscalar as a dilaton, we have presented the complete electroweak corrections to the corresponding interactions and we have discussed the renormalization properties of the same vertices. In particular, we have shown that the renormalizability of the dilaton vertices is inherited directly from that of the Standard Model only if the Higgs sector is characterized by a conformal coupling (χ) fixed at

the value $1/6$.

Then we have moved to an analysis of the analytic structure of the $J_D VV$ correlator, showing that it supports an anomaly pole as an interpolating state, which indicates that such a state can be interpreted as the Nambu-Goldstone (effective dilaton) mode of the anomalous breaking of the dilatation symmetry.

In fact, the trace anomaly seems to bring in some important information concerning the dynamics of the Standard Model, aspects that we have tried to elucidate. For this reason, we have extended a previous analysis of ours of the TVV vertex, performed in the broken electroweak phase and in QCD, in order to characterize the dynamical behaviour of the analogous $J_D VV$ correlator. The latter carries relevant information on the anomalous breaking of the dilatation symmetry in the Standard Model. In fact, as we move to high energy, far above the electroweak scale, the Lagrangian of the Standard Model becomes approximately scale-invariant. This approximate dilatation symmetry is broken by a quantum anomaly and its signature, as we have shown in our analysis, is in the appearance of an anomaly pole in the $J_D VV$ correlator. The same pole might appear in correlators with multiple insertions of J_D , but the proof of their existence is far more involved and requires further investigations. This pole is clearly massless in the perturbative picture, and accounts for the anomalous breaking of this approximate scale invariance.

Acknowledgments

We thank Pietro Colangelo for discussions. This work is supported by INFN of Italy under Iniziativa Specifica BARI-21.

A The coupling/decoupling of the anomaly pole

In perturbative QCD, the anomalous AVV diagram is characterized by the presence of an anomaly pole in the variable k^2 , with k denoting the momentum of the axial-vector current, which is explicitly shown in Eq.(65). It is interesting to note that this structure has a non-vanishing residue for on-shell photons and for massless quarks running in the loop. In this case the pole is said to be *infrared coupled*. This feature, supplemented by usual polology arguments, leads to a $\pi \rightarrow \gamma\gamma$ decay rate which is enhanced with respect to the non-anomalous case. On the other hand, if the photons are virtual or the quarks are massive the anomaly pole decouples, namely, its residue is zero. We refer to [8] for more details. The same behaviour is shared by the conformally anomalous TVV diagram [5]. We illustrate this important point in the QED case by considering the off-shell correlator.

We denote with s_1 and s_2 the virtualities of the two final state photons and with m the mass of the fermion running in the loops. The case with on-shell photons and a massive fermion has already been discussed in section 4.2. There we have shown that the anomaly pole has a non-vanishing residue only in the conformal limit, when all masses are set to zero. Indeed, in the case of a massive fermion, besides the fact that the anomaly pole anyway appears in the corresponding invariant amplitude $F_1(s; 0, 0, m^2)$, as one can see from Eq.(72), it will decouple, showing a zero residue

$$\lim_{s \rightarrow 0} s \Gamma^{\mu\nu\alpha\beta}(s; 0, 0, m^2) = 0. \quad (97)$$

As for the chiral anomaly case, the absence of the internal fermion masses is not sufficient to guarantee the infrared coupling of the anomaly pole. Indeed, if $m = 0$ but the photons are taken off-shell, being characterized by non zero virtualities s_1 and s_2 , one can check that the entire correlator is completely free from anomaly poles as

$$\lim_{s \rightarrow 0} s \Gamma^{\mu\nu\alpha\beta}(s; s_1, s_2, 0) = 0. \quad (98)$$

The computation of this limit needs the explicit results for all the invariant amplitudes F_i , which are not given here due to their lengthy expressions but can be found in [5] where the coupling/decoupling features of the TVV are discussed in more detail.

One should be aware of the fact that the same pole is present in the AVV diagram when VV are now the gluons. If the two gluons are on-shell, as in the 2-photon case, the perturbative anomaly pole is again infrared coupled. Obviously, such an enhancement is not observable, since the gluons cannot be on-shell, because of confinement. In the perturbative picture, a non-zero virtuality of the two gluons is then sufficient to exclude an infrared coupling of the anomaly pole.

B A classical scale invariant Lagrangian with a dilaton field

In this appendix we briefly describe the construction of a scale-invariant theory to clarify some of the issues concerning the coupling of a dilaton. In particular, the example has the goal to illustrate that in a classical scale-invariant extension of a given theory, the dilaton couples only to operators which are mass dependent, and thus scale breaking, before the extension. We take the case of a fundamental dilaton field (not a composite) introduced in this type of extensions.

A scale invariant extension of a given Lagrangian can be obtained if we promote all the dimensionfull constants to dynamical fields. We illustrate this point in the case of a simple interacting scalar field theory incorporating the Higgs mechanism. At a second stage we will derive the structure of the dilaton interaction at order $1/\Lambda$, where Λ is the scale characterizing the spontaneous breaking of the dilatation symmetry.

Our toy model consists in a real singlet scalar with a potential of the kind of $V_2(\phi)$ introduced in section 4,

$$\mathcal{L} = \frac{1}{2}(\partial\phi)^2 - V_2(\phi) = \frac{1}{2}(\partial\phi)^2 + \frac{\mu^2}{2}\phi^2 - \lambda\frac{\phi^4}{4} - \frac{\mu^4}{4\lambda}, \quad (99)$$

obeying the classical equation of motion

$$\square\phi = \mu^2\phi - \lambda\phi^3. \quad (100)$$

Obviously this theory is not scale invariant due to the appearance of the mass term μ . This feature is reflected in the trace of the EMT. Indeed the canonical EMT of such a theory and its trace are

$$\begin{aligned} T_c^{\mu\nu}(\phi) &= \partial^\mu\phi\partial^\nu\phi - \frac{1}{2}\eta^{\mu\nu}\left[(\partial\phi)^2 + \mu^2\phi^2 - \lambda\frac{\phi^4}{2} - \frac{\mu^4}{2\lambda}\right], \\ T_c^\mu{}_\mu(\phi) &= -(\partial\phi)^2 - 2\mu^2\phi^2 + \lambda\phi^4 + \frac{\mu^4}{\lambda}. \end{aligned} \quad (101)$$

It is well known that the EMT of a scalar field can be improved in such a way as to make its trace proportional only to the scale breaking parameter, i.e. the mass μ . This can be done by adding an extra contribution $T_I^{\mu\nu}(\phi, \chi)$ which is symmetric and conserved

$$T_I^{\mu\nu}(\phi, \chi) = \chi (\eta^{\mu\nu} \square \phi^2 - \partial^\mu \partial^\nu \phi^2) , \quad (102)$$

where the χ parameter is conveniently chosen. The combination of the canonical plus the improvement EMT, $T^{\mu\nu} \equiv T_c^{\mu\nu} + T_I^{\mu\nu}$ has the off-shell trace

$$T^\mu{}_\mu(\phi, \chi) = (\partial\phi)^2 (6\chi - 1) - 2\mu^2 \phi^2 + \lambda \phi^4 + \frac{\mu^4}{\lambda} + 6\chi \phi \square \phi . \quad (103)$$

Using the equation of motion (100) and choosing $\chi = 1/6$ the trace relation given above becomes proportional uniquely to the scale breaking term μ

$$T^\mu{}_\mu(\phi, 1/6) = -\mu^2 \phi^2 + \frac{\mu^4}{\lambda} . \quad (104)$$

The scale invariant extension of the Lagrangian given in Eq.(99) is achieved by promoting the mass terms to dynamical fields by the replacement

$$\mu \rightarrow \frac{\mu}{\Lambda} \Sigma , \quad (105)$$

obtaining

$$\mathcal{L} = \frac{1}{2} (\partial\phi)^2 + \frac{1}{2} (\partial\Sigma)^2 + \frac{\mu^2}{2\Lambda^2} \Sigma^2 \phi^2 - \lambda \frac{\phi^4}{4} - \frac{\mu^4}{4\lambda\Lambda^4} \Sigma^4 \quad (106)$$

where we have used Eq.(105) and introduced a kinetic term for the dilaton Σ . Obviously, the new Lagrangian is dilatation invariant, as one can see from the trace of the improved EMT

$$T^\mu{}_\mu(\phi, \Sigma, \chi, \chi') = (6\chi - 1) (\partial\phi)^2 + (6\chi' - 1) (\partial\Sigma)^2 + 6\chi \phi \square \phi + 6\chi' \Sigma \square \Sigma - 2 \frac{\mu^2}{\Lambda^2} \Sigma^2 \phi^2 + \lambda \phi^4 + \frac{1}{\lambda} \frac{\mu^4}{\Lambda^4} \Sigma^4 , \quad (107)$$

which vanishes upon using the equations of motion for the Σ and ϕ fields,

$$\begin{aligned} \square \phi &= \frac{\mu^2}{\Lambda^2} \Sigma^2 \phi - \lambda \phi^3 , \\ \square \Sigma &= \frac{\mu^2}{\Lambda^2} \Sigma \phi^2 - \frac{1}{\lambda} \frac{\mu^4}{\Lambda^4} \Sigma^3 , \end{aligned} \quad (108)$$

and setting the χ, χ' parameters at the special value $\chi = \chi' = 1/6$.

As we have already discussed in section 4, the scalar potential V_2 allows to perform the spontaneous breaking of the scale symmetry around a stable minimum point, giving the dilaton and the scalar field the vacuum expectation values Λ and v respectively

$$\Sigma = \Lambda + \rho , \quad \phi = v + h . \quad (109)$$

For our present purposes, it is enough to expand the Lagrangian (106) around the vev for the dilaton field, as we are interested in the structure of the couplings of its fluctuation ρ

$$\mathcal{L} = \frac{1}{2} (\partial\phi)^2 + \frac{1}{2} (\partial\rho)^2 + \frac{\mu^2}{2} \phi^2 - \lambda \frac{\phi^4}{4} - \frac{\mu^4}{4\lambda} - \frac{\rho}{\Lambda} \left(-\mu^2 \phi^2 + \frac{\mu^4}{\lambda} \right) + \dots , \quad (110)$$

where the ellipsis refer to terms that are higher order in $1/\Lambda$. It is clear, from (104) and (110), that one can write an dilaton Lagrangian at order $1/\Lambda$, as

$$\mathcal{L}_\rho = (\partial\rho)^2 - \frac{\rho}{\Lambda} T^\mu{}_\mu(\phi, 1/6) + \dots, \quad (111)$$

where the equations of motion have been used in the trace of the energy momentum tensor. Expanding the scalar field around v would render the previous equation more complicated and we omit it for definiteness. We only have to mention that a mixing term $\sim \rho h$ shows up and it has to be removed diagonalizing the mass matrix, switching from interaction to mass eigenstates exactly in the way we discussed in section 4, to which we refer for the details.

It is clear, from this simple analysis, that a dilaton, in general, does not couple to the anomaly, but only to the sources of explicit breaking of scale invariance, i.e. to the mass terms. The coupling of a dilaton to an anomaly is, on the other hand, necessary, if the state is interpreted as a composite pseudo Nambu-Goldstone mode of the dilatation symmetry. Thus, this coupling has to be introduced by hand, in strict analogy with the chiral case.

C Quantum conformal invariance and dilaton couplings at low energy

As a second example, we consider the situation in which all the SM fields are embedded in a (quantum) Conformal Field Theory (CFT) extension [11] and we discuss the (loop-induced) couplings of the dilaton to the massless gauge bosons. At tree level the dilaton of [11] couples to the SM fields only through their masses, as the fundamental dilaton which we have discussed previously, and, in this respect, it behaves like the SM Higgs, without scale anomaly contributions. For this reason the dilaton interaction with the massless gauge bosons is induced by quantum effects mediated by heavy particles running in the loops (in this context heavier or lighter is referred to the dilaton mass), and not by anomalous terms. When the mass m_i of the particle running in the loop is much greater than the dilaton mass, the coupling to the massless gauge bosons becomes

$$\mathcal{L}_\rho = \frac{\alpha_s}{8\pi} \sum_i b_g^i \frac{\rho}{\Lambda} (F_{g\mu\nu}^a)^2 + \frac{\alpha_{em}}{8\pi} \sum_i b_{em}^i \frac{\rho}{\Lambda} (F_{\gamma\mu\nu})^2, \quad (112)$$

where b_{em}^i and b_g^i are the contributions of the heavy field i to the one-loop β function (computed in the \overline{MS} scheme) for the electromagnetic and strong coupling constants respectively. The β functions are normalized as

$$\beta_i = \frac{g^3}{16\pi^2} b^i. \quad (113)$$

Note that this result is independent from the heavy mass m_i as one can prove by analyzing the structure of the mass corrections of the dilaton coupling, which reads as

$$\Gamma_{\rho VV} \sim \frac{g^2}{\pi^2 \Lambda} m_i^2 \left[\frac{1}{s} - \frac{1}{2} \mathcal{C}_0(s, 0, 0, m_i^2, m_i^2, m_i^2) \left(1 - \frac{4m_i^2}{s} \right) \right] \sim \frac{g^2}{\pi^2 \Lambda} \frac{1}{6} + O\left(\frac{s}{m_i^2}\right) \quad (114)$$

where $s = m_\rho^2$ is fixed at the dilaton mass and we have performed the large mass limit of the amplitude using

$$\mathcal{C}_0(s, 0, 0, m_i^2, m_i^2, m_i^2) \sim -\frac{1}{2m_i^2} \left(1 + \frac{1}{12} \frac{s}{m_i^2} + O\left(\frac{s^2}{m_i^4}\right) \right) \quad (115)$$

valid for $m_i^2 \gg s = m_\rho^2$. This shows that in the case of heavy fermions, the dependence on the fermion mass cancels. Obviously, this limit generates an effective coupling which is proportional to the β function related to the heavy flavours. The same reasonings can be employed to the Higgs case as well. It is clear that this coupling to the massless gauge bosons is dependent from new heavy states and, therefore, from the UV completion of the SM. This is certainly the case for the Standard Model Higgs whose double photon decay is one of the most important decay channel for new physics discoveries.

For the dilaton case the situation is slightly different. Surely we do not understand the details of the CFT extension, nor its particle spectrum, but nevertheless we know that the conformal symmetry is realized at the quantum level. Therefore the complete β functions, including the contribution from all states, must vanish

$$\beta = \frac{g^3}{16\pi^2} \left[\sum_i b^i + \sum_j b^j \right] = 0, \quad (116)$$

where i and j run over the heavy and light states respectively. Exploiting the consequence of the quantum conformal symmetry, the dilaton couplings to the massless gauge bosons become

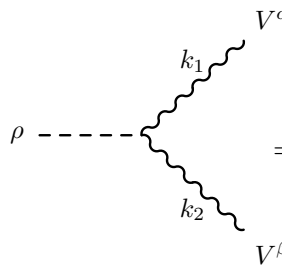
$$\mathcal{L}_\rho = -\frac{\alpha_s}{8\pi} \sum_j b_g^j \frac{\rho}{\Lambda} (F_{g\mu\nu}^a)^2 - \frac{\alpha_{em}}{8\pi} \sum_j b_{em}^j \frac{\rho}{\Lambda} (F_{\gamma\mu\nu})^2, \quad (117)$$

in which the dependence from the β functions of the light states is now explicit. We emphasize that the appearance of the light states contributions to the β functions is a consequence of the vanishing of the complete β , and, therefore, of the CFT extension and not the result of a direct coupling of the dilaton to the anomaly.

D Appendix. Feynman rules

The Feynman rules used throughout the paper are collected here. We have

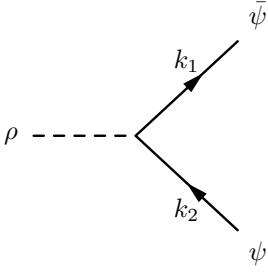
- dilaton - gauge boson - gauge boson vertex



$$= V_{\rho V V}^{\alpha\beta}(k_1, k_2) = -\frac{2i}{\Lambda} \left\{ M_V^2 \eta^{\alpha\beta} - \frac{1}{\xi} \left(k_1^\alpha k_1^\beta + k_2^\alpha k_2^\beta + 2 k_1^\alpha k_2^\beta \right) \right\} \quad (118)$$

where V stands for the gluons or for the vector gauge bosons A, Z and W^\pm and, if the gauge bosons are gluons, a color-conserving δ_{ab} matrix must be included.

- dilaton - fermion - fermion vertex

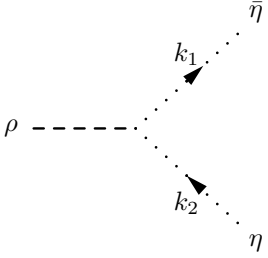


The diagram shows a vertex where a dashed line labeled ρ enters from the left. Two solid lines emerge from the vertex: one labeled $\bar{\psi}$ with momentum k_1 pointing away from the vertex, and another labeled ψ with momentum k_2 pointing away from the vertex.

$$= V_{\rho\bar{\psi}\psi}(k_1, k_2) = -\frac{i}{2\Lambda} \left\{ 3 (k_1 - k_2) + 8 m_f \right\} \quad (119)$$

If the fermions are quarks, the vertex must be multiplied by the identity color matrix δ_{ab} .

- dilaton - ghost - ghost vertex

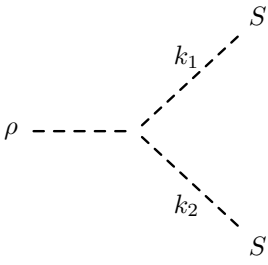


The diagram shows a vertex where a dashed line labeled ρ enters from the left. Two dotted lines emerge from the vertex: one labeled $\bar{\eta}$ with momentum k_1 pointing away from the vertex, and another labeled η with momentum k_2 pointing away from the vertex.

$$= V_{\rho\bar{c}c}(k_1, k_2) = -\frac{2i}{\Lambda} \left\{ k_1 \cdot k_2 + 2 M_\eta^2 \right\} \quad (120)$$

where η denotes both the QCD ghost fields c^a or the electroweak ghost fields η^+ , η^- and η^Z . In the QCD case one must include a color-conserving δ_{ab} matrix.

- dilaton - scalar - scalar vertex

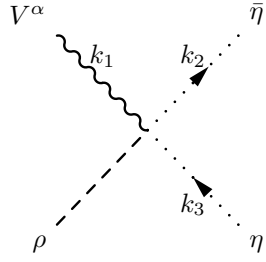


The diagram shows a vertex where a dashed line labeled ρ enters from the left. Two dashed lines emerge from the vertex: one labeled S with momentum k_1 pointing away from the vertex, and another labeled S with momentum k_2 pointing away from the vertex.

$$\begin{aligned} = V_{\rho SS}(k_1, k_2) &= -\frac{2i}{\Lambda} \left\{ k_1 \cdot k_2 + 2 M_S^2 \right\} \\ &= \frac{i}{\Lambda} 6 \chi (k_1 + k_2)^2 \end{aligned} \quad (121)$$

where S stands for the Higgs H and the Goldstones ϕ and ϕ^\pm . The first expression is the contribution coming from the minimal energy-momentum tensor while the second is due to the term of improvement.

- dilaton - gauge boson - ghost - ghost vertex

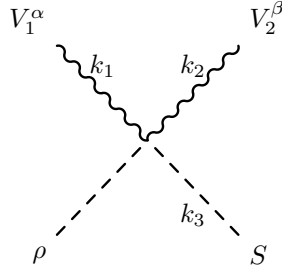


$$= V_{\rho V \bar{\eta} \eta}^\alpha(k_2) = -\frac{2i}{\Lambda} \mathcal{C}_{V\eta} k_2^\alpha \quad (125)$$

where V denotes the g^a , A , Z gauge bosons and η the ghosts c^b , η^+ , η^- . The coefficients \mathcal{C} are defined as

$$\mathcal{C}_{g^a c^b} = f^{abc} g \quad \mathcal{C}_{A\eta^+} = e \quad \mathcal{C}_{A\eta^-} = -e \quad \mathcal{C}_{Z\eta^+} = e \frac{c_w}{s_w} \quad \mathcal{C}_{Z\eta^-} = -e \frac{c_w}{s_w}.$$

- dilaton - gauge boson - gauge boson - scalar vertex

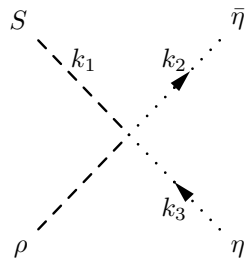


$$= V_{\rho V V S}^{\alpha\beta} = -\frac{2}{\Lambda} e \mathcal{C}_{V_1 V_2 S} M_W \eta^{\alpha\beta} \quad (126)$$

where V stands for A , Z and W^\pm and S for ϕ^\pm and H . The coefficients are defined as

$$\begin{aligned} \mathcal{C}_{AW^+\phi^-} &= 1 & \mathcal{C}_{AW^-\phi^+} &= -1 & \mathcal{C}_{ZW^+\phi^-} &= -\frac{s_w}{c_w} \\ \mathcal{C}_{ZW^-\phi^+} &= \frac{s_w}{c_w} & \mathcal{C}_{ZZH} &= -\frac{i}{s_w c_w^2} & \mathcal{C}_{W^+W^-H} &= -\frac{i}{c_w}. \end{aligned}$$

- dilaton - scalar - ghost - ghost vertex

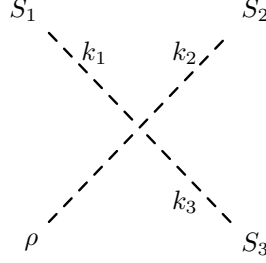


$$= V_{\rho S \bar{\eta} \eta} = -\frac{4i}{\Lambda} e \mathcal{C}_{S\eta} M_W \quad (127)$$

where $S = H$ and η denotes η^+ , η^- and η^z . The vertex is defined with the coefficients

$$\mathcal{C}_{H\eta^+} = \mathcal{C}_{H\eta^-} = \frac{1}{2s_w} \quad \mathcal{C}_{H\eta^z} = \frac{1}{2s_w c_w}.$$

- dilaton - three scalar vertex



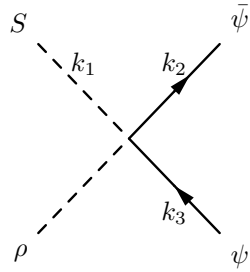
$$= V_{\rho SSS} = -\frac{4i}{\Lambda} e \mathcal{C}_{S_1 S_2 S_3}$$

(128)

with S denoting H , ϕ and ϕ^\pm . We have defined the coefficients

$$\mathcal{C}_{H\phi\phi} = \mathcal{C}_{H\phi^+\phi^-} = \frac{1}{2s_w c_w} \frac{M_H^2}{M_Z} \quad \mathcal{C}_{HHH} = \frac{3}{2s_w c_w} \frac{M_H^2}{M_Z}.$$

- dilaton - scalar - fermion - fermion vertex



$$= V_{\rho S \bar{\psi} \psi} = -\frac{2i}{\Lambda} \frac{e}{s_w c_w} \frac{m_f}{M_Z}$$

(129)

where S is only the Higgs scalar H .

- dilaton - gluon - fermion - fermion vertex

$$= V_{\rho g \bar{\psi} \psi}^a = \frac{3i}{\Lambda} g T^a \gamma^\alpha.$$

(130)

- dilaton - photon - fermion - fermion vertex

$$= V_{\rho \gamma \bar{\psi} \psi}^\alpha = Q_f e \frac{3i}{\Lambda} \gamma^\alpha$$

(131)

where Q_f is the fermion charge expressed in units of e .

- dilaton - Z - fermion - fermion vertex

$$= V_{\rho Z \bar{\psi} \psi}^\alpha = \frac{3i}{2\Lambda s_w c_w} e (C_v^f - C_a^f \gamma^5) \gamma^\alpha$$

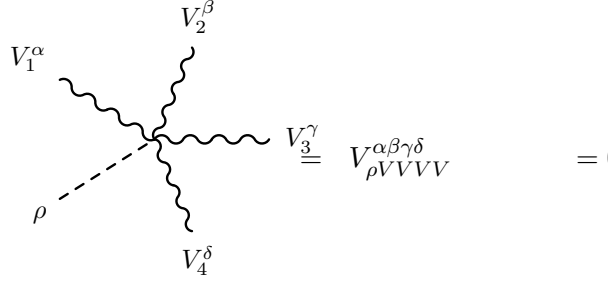
(132)

where C_v^f and C_a^f are the vector and axial-vector couplings of the Z gauge boson to the fermion (f). Their expressions are

$$C_v^f = I_3^f - 2s_w^2 Q^f \quad C_a^f = I_3^f.$$

I_3^f denotes the 3rd component of the isospin.

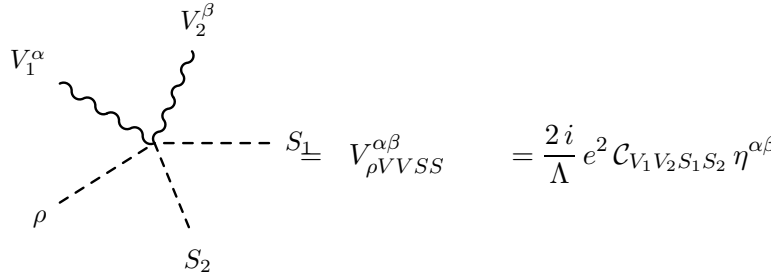
- dilaton - four gauge bosons vertex



$$V_1^\alpha \quad V_2^\beta \quad V_3^\gamma \quad V_4^\delta \quad \rho \quad V_{\rho VVVV}^{\alpha\beta\gamma\delta} = 0 \quad (133)$$

where V_1, V_2, V_3 and V_4 denote g, A, Z or W^\pm .

- dilaton - gauge boson - gauge boson - scalar - scalar vertex



$$V_1^\alpha \quad V_2^\beta \quad S_\perp \quad \rho \quad S_2 \quad V_{\rho VVSS}^{\alpha\beta} = \frac{2i}{\Lambda} e^2 \mathcal{C}_{V_1 V_2 S_1 S_2} \eta^{\alpha\beta} \quad (134)$$

where V_1 and V_2 denote the neutral gauge bosons A and Z , while the possible scalars are ϕ, ϕ^\pm and H . The coefficients are

$$\mathcal{C}_{AA\phi^+\phi^-} = 2 \quad \mathcal{C}_{AZ\phi^+\phi^-} = \frac{c_w^2 - s_w^2}{s_w c_w} \quad \mathcal{C}_{ZZ\phi^+\phi^-} = \frac{(c_w^2 - s_w^2)^2}{2s_w^2 c_w^2} \quad \mathcal{C}_{ZZ\phi\phi} = \mathcal{C}_{ZZHH} = \frac{1}{2s_w^2 c_w^2}.$$

E Appendix. The scalar integrals

We collect in this appendix the definition of the scalar integrals appearing in the computation of the correlators. One-, two- and three-point functions are denoted, respectively as $\mathcal{A}_0, \mathcal{B}_0$ and \mathcal{C}_0 , with

$$\begin{aligned} \mathcal{A}_0(m_0^2) &= \frac{1}{i\pi^2} \int d^n l \frac{1}{l^2 - m_0^2}, \\ \mathcal{B}_0(k^2, m_0^2, m_1^2) &= \frac{1}{i\pi^2} \int d^n l \frac{1}{(l^2 - m_0^2)((l+k)^2 - m_1^2)}, \\ \mathcal{C}_0((p+q)^2, p^2, q^2, m_0^2, m_1^2, m_2^2) &= \frac{1}{i\pi^2} \int d^n l \frac{1}{(l^2 - m_0^2)((l+p)^2 - m_1^2)((l-q)^2 - m_2^2)}. \end{aligned} \quad (135)$$

We have also used the finite combination of two-point scalar integrals

$$\mathcal{D}_0(p^2, q^2, m_0^2, m_1^2) = \mathcal{B}_0(p^2, m_0^2, m_1^2) - \mathcal{B}_0(q^2, m_0^2, m_1^2). \quad (136)$$

The explicit expressions of \mathcal{A}_0 , \mathcal{B}_0 and \mathcal{C}_0 can be found in [12].

F Appendix. Contributions to $\mathcal{V}_{\rho ZZ}$

• The fermion sector

$$\begin{aligned} \Phi_{ZZ}^F(p, q) = & \sum_f \left\{ \frac{\alpha m_f^2}{\pi s c_w^2 s_w^2 (s - 4M_Z^2)} (s - 2M_Z^2) (C_a^{f2} + C_v^{f2}) \right. \\ & + \frac{2\alpha m_f^2}{\pi s c_w^2 (s - 4M_Z^2)^2 s_w^2} \left[(2M_Z^4 - 3sM_Z^2 + s^2) C_a^{f2} + C_v^{f2} M_Z^2 (2M_Z^2 + s) \right] \mathcal{D}_0(s, M_Z^2, m_f^2, m_f^2) \\ & + \frac{\alpha m_f^2}{2\pi s c_w^2 (s - 4M_Z^2)^2 s_w^2} (s - 2M_Z^2) \{ [4M_Z^4 - 2(8m_f^2 + s) M_Z^2 + s(4m_f^2 + s)] C_a^{f2} \\ & + C_v^{f2} [4M_Z^4 + 2(3s - 8m_f^2) M_Z^2 - s(s - 4m_f^2)] \} \mathcal{C}_0(s, M_Z^2, M_Z^2, m_f^2, m_f^2, m_f^2) \} \end{aligned} \quad (137)$$

$$\begin{aligned} \Xi_{ZZ}^F(p, q) = & \sum_f \left\{ - \frac{\alpha m_f^2}{\pi s c_w^2 (s - 4M_Z^2) s_w^2} \left[(2M_Z^4 - 4sM_Z^2 + s^2) C_a^{f2} + 2C_v^{f2} M_Z^4 \right] \right. \\ & - \frac{\alpha m_f^2}{\pi c_w^2 s_w^2} C_a^{f2} \mathcal{B}_0(s, m_f^2, m_f^2) - \frac{2\alpha m_f^2 M_Z^2}{\pi s c_w^2 (s - 4M_Z^2)^2 s_w^2} [s^2 C_a^{f2} - 2(C_a^{f2} + C_v^{f2}) M_Z^4 \\ & + 2s(C_v^{f2} - C_a^{f2}) M_Z^2] \mathcal{D}_0(s, M_Z^2, m_f^2, m_f^2) \\ & - \frac{\alpha m_f^2}{\pi s c_w^2 (s - 4M_Z^2)^2 s_w^2} \left[4M_Z^8 - 2(8m_f^2 + 5s) M_Z^6 + 3s(12m_f^2 + s) M_Z^4 - 16s^2 m_f^2 M_Z^2 \right. \\ & \left. \left. + 2s^3 m_f^2 \right] C_a^{f2} + C_v^{f2} M_Z^4 [4M_Z^4 - 2(8m_f^2 + s) M_Z^2 + s(4m_f^2 + s)] \right] \mathcal{C}_0(s, M_Z^2, M_Z^2, m_f^2, m_f^2, m_f^2) \} \end{aligned} \quad (138)$$

• **The W boson sector**

$$\begin{aligned}
\Phi_{ZZ}^W(p, q) = & \frac{\alpha}{s_w^2 c_w^2 \pi} \left[\frac{M_Z^2}{2s(s-4M_Z^2)} [2M_Z^2(-12s_w^6 + 32s_w^4 - 29s_w^2 + 9) \right. \\
& \left. + s(12s_w^6 - 36s_w^4 + 33s_w^2 - 10)] \right] \\
& + \frac{\alpha M_Z^2}{2s_w^2 c_w^2 \pi s(s-4M_Z^2)^2} [4M_Z^4(12s_w^6 - 32s_w^4 + 29s_w^2 - 9) \\
& + 2M_Z^2 s(s_w^2 - 2)(12s_w^4 - 12s_w^2 + 1) + s^2(-4s_w^4 + 8s_w^2 - 5)] \mathcal{D}_0(s, M_Z^2, M_W^2, M_W^2) \\
& + \frac{\alpha M_Z^2}{2\pi s_w^2 c_w^2 s(s-4M_Z^2)^2} \left[-4M_Z^6(s_w^2 - 1)(4s_w^2 - 3)(12s_w^4 - 20s_w^2 + 9) \right. \\
& + 2M_Z^4 s(18s_w^4 - 34s_w^2 + 15)(4(s_w^2 - 3)s_w^2 + 7) - 2M_Z^2 s^2(12s_w^8 - 96s_w^6 + 201s_w^4 - 157s_w^2 + 41) + \\
& \left. s^3(-12s_w^6 + 32s_w^4 - 27s_w^2 + 7) \right] \mathcal{C}_0(s, M_Z^2, M_Z^2, M_W^2, M_W^2, M_W^2) \quad (139)
\end{aligned}$$

$$\begin{aligned}
\Xi_{ZZ}^W(p, q) = & \frac{\alpha M_Z^2}{2\pi s_w^2 c_w^2 s(s-4M_Z^2)} \left[2M_Z^4(-12s_w^6 + 32s_w^4 - 29s_w^2 + 9) \right. \\
& \left. + sM_Z^2[4(s_w^4 + s_w^2) - 7] - 2s^2(s_w^2 - 1) \right] + \frac{\alpha M_Z^2}{\pi s_w^2 c_w^2} (-2s_w^4 + 3s_w^2 - 1) \mathcal{B}_0(s, M_W^2, M_W^2) \\
& + \frac{\alpha M_Z^2}{\pi s_w^2 c_w^2 s(s-M_Z^2)^2} [2M_Z^6(12s_w^6 - 32s_w^4 + 29s_w^2 - 9) + sM_Z^4(-24s_w^6 + 92s_w^4 - 110s_w^2 + 41) \\
& + s^2 M_Z^2(-12s_w^4 + 26s_w^2 - 13) + 2s^3(s_w^2 - 1)^2] \mathcal{D}_0(s, M_Z^2, M_W^2, M_W^2) \\
& + \frac{\alpha M_Z^2}{4\pi s_w^2 c_w^2 s(s-M_Z^2)^2} [-8M_Z^8(s_w^2 - 1)(4s_w^2 - 3)(12s_w^4 - 20s_w^2 + 9) \\
& + 4sM_Z^6(24s_w^8 - 60s_w^6 + 30s_w^4 + 25s_w^2 - 18) + 2s^2 M_Z^4(-20s_w^6 + 76s_w^4 - 103s_w^2 + 46) \\
& + s^3 M_Z^2(-4s_w^4 + 24s_w^2 - 19) - 2s^4(s_w^2 - 1)] \mathcal{C}_0(s, M_Z^2, M_Z^2, M_W^2, M_W^2, M_W^2) \quad (140)
\end{aligned}$$

• **The (Z, H) sector**

$$\begin{aligned}
\Phi_{ZZ}^{ZH}(p, q) = & \frac{-\alpha}{4\pi s c_w^2 s_w^2 (s-4M_Z^2)} \left\{ [M_H^2(s-2M_Z^2) + 3sM_Z^2 - 2M_Z^4] \right. \\
& + 2(M_Z^2 - M_H^2)(\mathcal{A}_0(M_Z^2) - \mathcal{A}_0(M_H^2)) \\
& + \frac{1}{(s-4M_Z^2)} [2M_H^2(sM_Z^2 - 2M_Z^4 + s^2) + 3s^2 M_Z^2 - 14sM_Z^4 + 8M_Z^6] \mathcal{B}_0(s, M_Z^2, M_Z^2) \\
& - \frac{1}{(s-4M_Z^2)} (2M_H^2 + s) [2M_H^2(s-M_Z^2) - 3sM_Z^2] \mathcal{B}_0(s, M_H^2, M_H^2) \\
& + \frac{2}{(s-4M_Z^2)} [sM_H^4 + 6(s-M_H^2)M_Z^4 + (2M_H^4 - 3sM_H^2 - 3s^2)M_Z^2] \mathcal{B}_0(M_Z^2, M_Z^2, M_H^2) \\
& + \frac{(2M_H^2 + s)}{(s-4M_Z^2)} \left[M_Z^2(-8sM_H^2 - 2M_H^4 + s^2) + 2M_Z^4(4M_H^2 + s) + 2sM_H^4 \right] \mathcal{C}_0(s, M_Z^2, M_Z^2, M_Z^2, M_H^2, M_H^2) \\
& \left. + \frac{M_H^2}{(s-4M_Z^2)} [2M_H^2(sM_Z^2 - 2M_Z^4 + s^2) - 20sM_Z^4 + 16M_Z^6 + s^3] \mathcal{C}_0(s, M_Z^2, M_Z^2, M_H^2, M_Z^2, M_Z^2) \right\} \quad (141)
\end{aligned}$$

$$\begin{aligned}
\Xi_{ZZ}^{ZH}(p, q) = & -\frac{\alpha}{8\pi s c_w^2 s_w^2 (s - 4M_Z^2)} \left\{ -4M_Z^2 (M_Z^4 + M_H^2 M_Z^2 - 3sM_Z^2 + s^2) \right. \\
& + 2(M_H^2 - M_Z^2)(s - 2M_Z^2)(\mathcal{A}_0(M_Z^2) - \mathcal{A}_0(M_H^2)) \\
& - \frac{1}{(s - 4M_Z^2)} [(8M_Z^6 + s^3) M_H^2 + M_Z^2 (s - 4M_Z^2)(s - 2M_Z^2)(3s - 2M_Z^2)] \mathcal{B}_0(s, M_Z^2, M_Z^2) \\
& + \frac{1}{(s - 4M_Z^2)} [2(4M_H^4 - s^2) M_Z^4 - s(2M_H^2 + s)^2 M_Z^2 + s^2 M_H^2 (2M_H^2 + s)] \mathcal{B}_0(s, M_H^2, M_H^2) \\
& + \frac{8M_Z^2}{(s - 4M_Z^2)} [-sM_H^4 - (3M_H^2 + 5s) M_Z^4 + (M_H^2 + s)(M_H^2 + 2s) M_Z^2] \mathcal{B}_0(M_Z^2, M_Z^2, M_H^2) \\
& - \frac{(2M_H^2 + s)}{(s - 4M_Z^2)} [4(7s - 4M_H^2) M_Z^6 + 4(M_H^2 - s)(M_H^2 + 3s) M_Z^4 \\
& + 2s(-M_H^4 - 2sM_H^2 + s^2) M_Z^2 + s^2 M_H^4] \mathcal{C}_0(s, M_Z^2, M_Z^2, M_Z^2, M_H^2, M_H^2) \\
& - \frac{1}{(s - 4M_Z^2)} [(8M_Z^6 + s^3) M_H^4 \\
& + 4M_Z^2 (s - 4M_Z^2)(2M_Z^4 - sM_Z^2 + s^2) M_H^2 \\
& + 4sM_Z^4 (s - 4M_Z^2)^2] \mathcal{C}_0(s, M_Z^2, M_Z^2, M_H^2, M_Z^2, M_Z^2) \left. \right\} \quad (142)
\end{aligned}$$

• **Term of improvement**

$$\begin{aligned}
\Phi_{ZZ}^I(p, q) = & \frac{3\chi\alpha}{2\pi s_w^2 c_w^2 (s - 4M_Z^2)^2} \left\{ (c_w^2 - s_w^2)^2 \left[2M_Z^2 s - 8M_Z^4 \right. \right. \\
& + 2M_Z^2 (s + 2M_Z^2) \mathcal{D}_0(s, M_Z^2, M_W^2, M_W^2) + 2(c_w^2 M_Z^2 (8M_Z^4 - 6M_Z^2 s + s^2) - 2M_Z^6 + 2M_Z^4 s) \\
& \times \mathcal{C}_0(s, M_Z^2, M_Z^2, M_W^2, M_W^2, M_W^2) \left. \right] + 2M_Z^2 s - 8M_Z^4 + 2M_Z^2 (s + 2M_Z^2) [\mathcal{B}_0(s, M_Z^2, M_Z^2) \\
& - \mathcal{B}_0(M_Z^2, M_Z^2, M_H^2)] + (3M_Z^2 s - 2M_H^2 (s - M_Z^2)) [\mathcal{B}_0(s, M_H^2, M_H^2) - \mathcal{B}_0(s, M_Z^2, M_Z^2)] \\
& + M_H^2 (2M_H^2 (s - M_Z^2) + 8M_Z^4 - 6M_Z^2 s + s^2) \mathcal{C}_0(s, M_Z^2, M_Z^2, M_H^2, M_Z^2, M_Z^2) \\
& + (2M_H^2 (M_H^2 - 4M_Z^2)(s - M_Z^2) + sM_Z^2 (s + 2M_Z^2)) \mathcal{C}_0(s, M_Z^2, M_Z^2, M_Z^2, M_H^2, M_H^2) \left. \right\} \quad (143)
\end{aligned}$$

$$\begin{aligned}
\Xi_{ZZ}^I(p, q) = & -\frac{3\chi\alpha s}{8\pi s_w^2 c_w^2 (s - 4M_Z^2)^2} \left\{ (c_w^2 - s_w^2)^2 \left[4M_Z^4 (s - 4M_Z^2) \right. \right. \\
& + 8M_Z^4 (s - M_Z^2) \mathcal{D}_0(s, M_Z^2, M_W^2, M_W^2) \\
& + 2M_Z^4 [s^2 - 2M_Z^2 s + 4M_Z^4 + 4c_w^2 M_Z^2 (s - 4M_Z^2)] \mathcal{C}_0(s, M_Z^2, M_Z^2, M_W^2, M_W^2, M_W^2) \left. \right] \\
& + 4M_Z^2 s_w^4 c_w^2 s (s - 4M_Z^2)^2 \mathcal{C}_0(s, M_Z^2, M_Z^2, M_W^2, M_W^2, M_W^2) + 4M_Z^2 (s - 4M_Z^2) \\
& + [M_Z^2 s (s + 2M_Z^2) - M_H^2 (s^2 - 2M_Z^2 s + 4M_Z^4)] [\mathcal{B}_0(s, M_H^2, M_H^2) - \mathcal{B}_0(s, M_Z^2, M_Z^2)] \\
& + 8M_Z^4 (s - M_Z^2) [\mathcal{B}_0(s, M_Z^2, M_Z^2) - \mathcal{B}_0(M_Z^2, M_Z^2, M_H^2)] + M_H^2 [4M_Z^4 (s - 4M_Z^2) \\
& + M_H^2 (s^2 - 2M_Z^2 s + 4M_Z^4)] \mathcal{C}_0(s, M_Z^2, M_Z^2, M_H^2, M_Z^2, M_Z^2) + [M_H^2 (M_H^2 - 4M_Z^2)(s^2 - 2M_Z^2 s + 4M_Z^4) \\
& + 2M_Z^2 s (s^2 - 6M_Z^2 s + 14M_Z^4)] \mathcal{C}_0(s, M_Z^2, M_Z^2, M_Z^2, M_H^2, M_H^2) \left. \right\}. \quad (144)
\end{aligned}$$

• **External leg corrections**

The $\Delta^{\alpha\beta}(p, q)$ correlator is decomposed as

$$\begin{aligned}\Delta^{\alpha\beta}(p, q) &= \left[\Sigma_{Min, \rho H}(k^2) + \Sigma_{I, \rho H}(k^2) \right] \frac{1}{s - M_H^2} V_{HZZ}^{\alpha\beta} + \left(\frac{\Lambda}{i} \right) V_{I, \rho H}(k) \frac{1}{s - M_H^2} \Sigma_{HH}(k^2) \frac{1}{s - M_H^2} V_{HZZ}^{\alpha\beta} \\ &+ \Delta_{I, HZZ}^{\alpha\beta}(p, q)\end{aligned}\quad (145)$$

where $\Sigma_{HH}(k^2)$ is the Higgs self-energy, $V_{HZZ}^{\alpha\beta}$ and $V_{I, \rho H}$ are tree level vertices defined in appendix (D) and $\Delta_{I, HZZ}^{\alpha\beta}(p, q)$ is expanded into the three contributions of improvement as

$$\begin{aligned}\Delta_{I, HZZ}^{\alpha\beta} &= \Delta_{(F), HZZ}^{\alpha\beta}(p, q) + \Delta_{(W), HZZ}^{\alpha\beta}(p, q) + \Delta_{(Z, H), HZZ}^{\alpha\beta}(p, q) \\ &= \left[\left(\frac{s}{2} - M_Z^2 \right) \eta^{\alpha\beta} - q^\alpha p^\beta \right] \Phi_{ZZ}^\Delta(p, q) + \eta^{\alpha\beta} \Xi_{ZZ}^\Delta(p, q) \\ &= \left[\left(\frac{s}{2} - M_Z^2 \right) \eta^{\alpha\beta} - q^\alpha p^\beta \right] \left(\Phi_{ZZ}^{\Delta F}(p, q) + \Phi_{ZZ}^{\Delta W}(p, q) + \Phi_{ZZ}^{\Delta W}(p, q) \right) \\ &\quad + \eta^{\alpha\beta} \left(\Xi_{ZZ}^{\Delta F}(p, q) + \Xi_{ZZ}^{\Delta W}(p, q) + \Xi_{ZZ}^{\Delta W}(p, q) \right).\end{aligned}\quad (146)$$

These are given by

$$\begin{aligned}\Phi_{ZZ}^{\Delta F}(p, q) &= - \sum_f \frac{6 \alpha \chi m_f^2}{\pi s_w^2 c_w^2 (s - M_H^2)(s - 4M_Z^2)} \left\{ (C_v^{f2} + C_a^{f2})(s - 2M_Z^2) \right. \\ &+ \frac{2}{s - 4M_Z^2} [M_Z^2(C_v^{f2} + C_a^{f2})(s + 2M_Z^2) + C_a^{f2}(s - 4M_Z^2)s] \mathcal{D}_0(s, M_Z^2, m_f^2, m_f^2) \\ &+ \frac{s - 2M_Z^2}{2(s - 4M_Z^2)} [(C_v^{f2} + C_a^{f2})(4m_f^2(s - 4M_Z^2) + 4M_Z^4 + 6M_Z^2 s - s^2) + 2C_a^{f2}s(s - 4M_Z^2)] \times \\ &\left. \mathcal{C}_0(s, M_Z^2, M_Z^2, m_f^2, m_f^2, m_f^2) \right\},\end{aligned}\quad (147)$$

$$\begin{aligned}\Xi_{ZZ}^{\Delta F}(p, q) &= \sum_f \frac{18 \alpha s \chi m_f^2}{\pi s_w^2 c_w^2 (s - M_H^2)(s - 4M_Z^2)} \eta^{\alpha\beta} \left\{ 2M_Z^2(C_v^{f2} + C_a^{f2}) \right. \\ &+ 2s(s - 4M_Z^2)C_a^{f2}\mathcal{B}_0(s, m_f^2, m_f^2) + \frac{2}{s - 4M_Z^2} [2M_Z^4(C_v^{f2} + C_a^{f2})(s - M_Z^2) + C_a^{f2}M_Z^2(s - 4M_Z^2)s] \times \\ &\mathcal{D}_0(s, M_Z^2, m_f^2, m_f^2) + \frac{1}{s - 4M_Z^2} [(C_v^{f2} + C_a^{f2})M_Z^4(4m_f^2(s - 4M_Z^2) + 4M_Z^4 - 2M_Z^2 s + s^2) \\ &\left. + 2C_a^{f2}s(s - 4M_Z^2)(m_f^2(s - 4M_Z^2) + M_Z^4)] \mathcal{C}_0(s, M_Z^2, M_Z^2, m_f^2, m_f^2, m_f^2) \right\}\end{aligned}\quad (148)$$

$$\begin{aligned}
\Phi_{ZZ}^{\Delta W}(p, q) = & \frac{3\alpha\chi}{\pi s_w^2 c_w^2 (s - M_H^2)(s - 4M_Z^2)} \left\{ \frac{s - 2M_Z^2}{2} [M_H^2(1 - 2s_w^2)^2 \right. \\
& + 2M_Z^2(-12s_w^6 + 32s_w^4 - 29s_w^2 + 9)] + \frac{M_Z^2}{s - 4M_Z^2} [M_H^2(1 - 2s_w^2)^2(s + 2M_Z^2) \\
& - 2(s_w^2 - 1)(2M_Z^4(12s_w^4 - 20s_w^2 + 9) + sM_Z^2(12s_w^4 - 20s_w^2 + 1) + 2s^2)] \mathcal{D}_0(s, M_Z^2, M_W^2, M_W^2) \\
& + \frac{M_Z^2}{s - 4M_Z^2} [2(s_w^2 - 1)(2M_Z^6(4s_w^2 - 3)(12s_w^4 - 20s_w^2 + 9) + 2M_Z^4 s(-36s_w^6 + 148s_w^4 - 163s_w^2 + 54) \\
& + M_Z^2 s^2(12s_w^6 - 96s_w^4 + 125s_w^2 - 43) + 4s^3(2s_w^4 - 3s_w^2 + 1)) - M_H^2(1 - 2s_w^2)^2(M_Z^4(8s_w^2 - 6) \\
& + 2M_Z^2 s(2 - 3s_w^2) + s^2(s_w^2 - 1))] \mathcal{C}_0(s, M_Z^2, M_Z^2, M_W^2, M_W^2, M_W^2) \left. \right\}, \tag{149}
\end{aligned}$$

$$\begin{aligned}
\Xi_{ZZ}^{\Delta W}(p, q) = & \frac{3\alpha\chi M_Z^2}{\pi s_w^2 c_w^2 (s - M_H^2)(s - 4M_Z^2)} \left\{ -M_Z^2[M_H^2(1 - 2s_w^2)^2 + 2M_Z^2(-12s_w^6 + 32s_w^4 - 29s_w^2 + 9)] \right. \\
& + \frac{s(s - 4M_Z^2)}{2} (8s_w^4 - 13s_w^2 + 5) \mathcal{B}_0(s, M_W^2, M_W^2) + \frac{2}{s - 4M_Z^2} [M_H^2 M_Z^2(1 - 2s_w^2)^2(M_Z^2 - s) \\
& - 2(s_w^2 - 1)(M_Z^6(12s_w^4 - 20s_w^2 + 9) - 3M_Z^4 s(4s_w^2 - 3)s_w^2 + 7) + M_Z^2 s^2(7 - 8s_w^2) + s^3(s_w^2 - 1)] \times \\
& \mathcal{D}_0(s, M_Z^2, M_W^2, M_W^2) + \frac{1}{2(s - 4M_Z^2)} [M_H^2(-4M_Z^6(1 - 2s_w^2)^2(4s_w^2 - 3) + 2M_Z^4 s(24s_w^6 - 28s_w^4 + 6s_w^2 - 1) \\
& + M_Z^2 s^2(-16s_w^6 + 12s_w^4 + 4s_w^2 - 1) + 2s^3 s_w^4(s_w^2 - 1)) + 2(s_w^2 - 1)(4M_Z^8(4s_w^2 - 3)(12s_w^4 - 20s_w^2 + 9) \\
& - 2M_Z^6 s(24s_w^6 - 52s_w^4 + 6s_w^2 + 15) + M_Z^4 s^2(45 - 4s_w^2(s_w^2 + 13)) + 2M_Z^2 s^3(4s_w^4 + 2s_w^2 - 5) \\
& - s^4(s_w^4 - 1))] \mathcal{C}_0(s, M_Z^2, M_Z^2, M_W^2, M_W^2, M_W^2) \left. \right\} \tag{150}
\end{aligned}$$

$$\begin{aligned}
\Phi_{ZZ}^{\Delta ZH}(p, q) = & \frac{\alpha\chi}{\pi s_w^2 c_w^2 (s - M_H^2)(s - 4M_Z^2)} \left\{ (2M_H^2 + M_Z^2)(s - 2M_Z^2) \right. \\
& - 2(M_H^2 - M_Z^2)(\mathcal{A}_0(M_Z^2) - \mathcal{A}_0(M_H^2)) + \frac{1}{s - 4M_Z^2} [2M_H^4(s - M_Z^2) + 3M_H^2 M_Z^2 s \\
& + 2M_Z^2(4M_Z^4 - 9M_Z^2 s + 2s^2)] \mathcal{B}_0(s, M_Z^2, M_Z^2) - \frac{3}{s - 4M_Z^2} [2M_H^4(s - M_Z^2) - 3M_H^2 M_Z^2 s] \mathcal{B}_0(s, M_H^2, M_H^2) \\
& - \frac{2}{s - 4M_Z^2} [M_H^2(s + 2M_Z^2)(4M_Z^2 - M_H^2) + 2M_Z^2 s(s - 4M_Z^2)] \mathcal{B}_0(M_Z^2, M_Z^2, M_H^2) \\
& - \frac{3M_H^2}{s - 4M_Z^2} [2M_H^2(s - M_Z^2)(4M_Z^2 - M_H^2) - M_Z^2 s(s + 2M_Z^2)] \mathcal{C}_0(s, M_Z^2, M_Z^2, M_Z^2, M_H^2, M_H^2) + \frac{M_H^2}{s - 4M_Z^2} \times \\
& [2M_H^4(s - M_Z^2) + M_H^2(4M_Z^4 - 2M_Z^2 s + s^2) + 2M_Z^2(8M_Z^4 - 14M_Z^2 s + 3s^2)] \mathcal{C}_0(s, M_Z^2, M_Z^2, M_H^2, M_Z^2, M_Z^2) \left. \right\} \tag{151}
\end{aligned}$$

$$\begin{aligned}
\Xi_{ZZ}^{\Delta ZH}(p, q) = & -\frac{3\alpha\chi}{\pi s_w^2 c_w^2 (s - M_H^2)(s - 4M_Z^2)} \left\{ M_Z^4(2M_H^2 + M_Z^2) \right. \\
& + \frac{1}{2}(M_Z^2 - M_H^2)(s - 2M_Z^2)(\mathcal{A}_0(M_Z^2) - \mathcal{A}_0(M_H^2)) + \frac{1}{4(s - 4M_Z^2)} [M_H^4(4M_Z^4 - 2M_Z^2s + s^2) \\
& + M_H^2M_Z^2s(s + 2M_Z^2) - M_Z^2(16M_Z^6 - 28M_Z^4s + 18M_Z^2s^2 - 3s^3)] \mathcal{B}_0(s, M_Z^2, M_Z^2) \\
& - \frac{3M_H^2}{4(s - 4M_Z^2)} [M_H^2(4M_Z^4 - 2M_Z^2s + s^2) - M_Z^2s(s + 2M_Z^2)] \mathcal{B}_0(s, M_H^2, M_H^2) \\
& + \frac{2}{s - 4M_Z^2} [M_Z^2s(M_H^2 - 2M_Z^2)^2 - M_H^2M_Z^4(M_H^2 - 4M_Z^2) - M_Z^4s^2] \mathcal{B}_0(M_Z^2, M_Z^2, M_H^2) \\
& + \frac{3M_H^2}{4(s - 4M_Z^2)} \times [M_H^2(4M_Z^4 - 2M_Z^2s + s^2)(M_H^2 - 4M_Z^2) + 2M_Z^2s(16M_Z^4 - 6M_Z^2s + s^2)] \times \\
& \mathcal{C}_0(s, M_Z^2, M_Z^2, M_Z^2, M_H^2, M_H^2) + \frac{1}{4(s - 4M_Z^2)} [M_H^6(4M_Z^4 - 2M_Z^2s + s^2) + 2M_H^4M_Z^2(s^2 - 4M_Z^4) \\
& - 4M_H^2M_Z^2(8M_Z^6 - 10M_Z^4s + 6M_Z^2s^2 - s^3) + 4M_Z^4s(s - 4M_Z^2)^2] \mathcal{C}_0(s, M_Z^2, M_Z^2, M_H^2, M_Z^2, M_Z^2) \left. \right\} \quad (152)
\end{aligned}$$

$$\begin{aligned}
\Sigma_{Min, \rho H}(k^2) = & \frac{e}{48\pi^2 s_w c_w M_Z} \left\{ \sum_f m_f^2 \left[3(4m_f^2 - k^2) \mathcal{B}_0(k^2, m_f^2, m_f^2) + 12\mathcal{A}_0(m_f^2) - 2k^2 + 12m_f^2 \right] \right. \\
& - \frac{1}{2} \left[3(k^2(M_H^2 - 6M_W^2) + 2M_W^2(M_H^2 + 6M_W^2)) \mathcal{B}_0(k^2, M_W^2, M_W^2) + 6(M_H^2 + 6M_W^2) \mathcal{A}_0(M_W^2) \right. \\
& - k^2(M_H^2 + 18M_W^2) + 6M_W^2(M_H^2 - 2M_W^2) \left. \right] - \frac{1}{4} \left[3(M_H^2(2M_Z^2 + s) + 12M_Z^4 - 6M_Z^2s) \right. \\
& \times \mathcal{B}_0(s, M_Z^2, M_Z^2) + 9M_H^2(2M_H^2 + s) \mathcal{B}_0(s, M_H^2, M_H^2) + 6(M_H^2 + 6M_Z^2) \mathcal{A}_0(M_Z^2) + 18M_H^2 \mathcal{A}_0(M_H^2) \\
& + 2(9M_H^4 + M_H^2(3M_Z^2 - 2s) - 6M_Z^4 - 9M_Z^2s) \left. \right] \left. \right\} \quad (153)
\end{aligned}$$

$$\Sigma_{I, \rho H}(k^2) = \frac{3e}{16\pi^2 s_w c_w} \frac{k^2 M_H^2}{M_Z^2} \chi \left[\mathcal{B}_0(k^2, M_W^2, M_W^2) + \frac{3}{2} \mathcal{B}_0(k^2, M_H^2, M_H^2) + \frac{1}{2} \mathcal{B}_0(k^2, M_Z^2, M_Z^2) \right] \quad (154)$$

G Appendix. Standard Model self-energies

We report here the expressions of the self-energies appearing in Section 2.4 which define the renormalization conditions. They are given by

$$\begin{aligned}
\Sigma_T^{\gamma}(p^2) = & -\frac{\alpha}{4\pi} \left\{ \frac{2}{3} \sum_f N_C^f 2Q_f^2 \left[-(p^2 + 2m_f^2) B_0(p^2, m_f^2, m_f^2) + 2m_f^2 B_0(0, m_f^2, m_f^2) + \frac{1}{3} p^2 \right] \right. \\
& + \left[(3p^2 + 4M_W^2) B_0(p^2, M_W^2, M_W^2) - 4M_W^2 B_0(0, M_W^2, M_W^2) \right] \left. \right\} \quad (155)
\end{aligned}$$

$$\begin{aligned}
\Sigma_T^{ZZ}(p^2) = & -\frac{\alpha}{4\pi} \left\{ \frac{2}{3} \sum_f N_C^f \left[\frac{C_V^{f2} + C_A^{f2}}{2s_w^2 c_w^2} \left(-(p^2 + 2m_f^2) B_0(p^2, m_f^2, m_f^2) + 2m_f^2 B_0(0, m_f^2, m_f^2) + \frac{1}{3} p^2 \right) \right. \right. \\
& + \left. \frac{3}{4s_w^2 c_w^2} m_f^2 B_0(p^2, m_f^2, m_f^2) \right] + \frac{1}{6s_w^2 c_w^2} \left[\left((18c_w^4 + 2c_w^2 - \frac{1}{2}) p^2 + (24c_w^4 + 16c_w^2 - 10) M_W^2 \right) \right. \\
& \times \left. B_0(p^2, M_W^2, M_W^2) - (24c_w^4 - 8c_w^2 + 2) M_W^2 B_0(0, M_W^2, M_W^2) + (4c_w^2 - 1) \frac{p^2}{3} \right] \\
& + \frac{1}{12s_w^2 c_w^2} \left[(2M_H^2 - 10M_Z^2 - p^2) B_0(p^2, M_Z^2, M_H^2) - 2M_Z^2 B_0(0, M_Z^2, M_Z^2) - 2M_H^2 B_0(0, M_H^2, M_H^2) \right. \\
& \left. \left. - \frac{(M_Z^2 - M_H^2)^2}{p^2} (B_0(p^2, M_Z^2, M_H^2) - B_0(0, M_Z^2, M_H^2)) - \frac{2}{3} p^2 \right] \right\} \quad (156)
\end{aligned}$$

$$\begin{aligned}
\Sigma_T^{\gamma Z}(p^2) = & \frac{\alpha}{4\pi s_w c_w} \left\{ \frac{2}{3} \sum_f N_C^f Q_f C_V^f \left[(p^2 + 2m_f^2) B_0(p^2, m_f^2, m_f^2) - 2m_f^2 B_0(0, m_f^2, m_f^2) - \frac{1}{3} p^2 \right] \right. \\
& \left. - \frac{1}{3} \left[\left((9c_w^2 + \frac{1}{2}) p^2 + (12c_w^2 + 4) M_W^2 \right) B_0(p^2, M_W^2, M_W^2) - (12c_w^2 - 2) M_W^2 B_0(0, M_W^2, M_W^2) + \frac{1}{3} p^2 \right] \right\} \quad (157)
\end{aligned}$$

$$\begin{aligned}
\Sigma_{HH}(p^2) = & -\frac{\alpha}{4\pi} \left\{ \sum_f N_C^f \frac{m_f^2}{2s_w^2 M_W^2} \left[2\mathcal{A}_0(m_f^2) + (4m_f^2 - p^2) \mathcal{B}_0(p^2, m_f^2, m_f^2) \right] \right. \\
& - \frac{1}{2s_w^2} \left[\left(6M_W^2 - 2p^2 + \frac{M_H^4}{2M_W^2} \right) \mathcal{B}_0(p^2, M_W^2, M_W^2) + \left(3 + \frac{M_H^2}{2M_W^2} \right) \mathcal{A}_0(M_W^2) - 6M_W^2 \right] \\
& - \frac{1}{4s_w^2 c_w^2} \left[\left(6M_Z^2 - 2p^2 + \frac{M_H^4}{2M_Z^2} \right) \mathcal{B}_0(p^2, M_Z^2, M_Z^2) + \left(3 + \frac{M_H^2}{2M_Z^2} \right) \mathcal{A}_0(M_Z^2) - 6M_Z^2 \right] \\
& \left. - \frac{3}{8s_w^2} \left[3 \frac{M_H^4}{M_W^2} \mathcal{B}_0(p^2, M_H^2, M_H^2) + \frac{M_H^2}{M_W^2} \mathcal{A}_0(M_H^2) \right] \right\} \quad (158)
\end{aligned}$$

$$\begin{aligned}
\Sigma_T^{WW}(p^2) = & -\frac{\alpha}{4\pi} \left\{ \frac{1}{3s_w^2} \sum_i \left[\left(\frac{m_{l,i}^2}{2} - p^2 \right) \mathcal{B}_0(p^2, 0, m_{l,i}^2) + \frac{p^2}{3} + m_{l,i}^2 \mathcal{B}_0(0, m_{l,i}^2, m_{l,i}^2) \right. \right. \\
& + \frac{m_{l,i}^4}{2p^2} (\mathcal{B}_0(p^2, 0, m_{l,i}^2) - \mathcal{B}_0(0, 0, m_{l,i}^2)) \left. \right] + \frac{1}{s_w^2} \sum_{i,j} |V_{ij}|^2 \left[\left(\frac{m_{u,i}^2 + m_{d,j}^2}{2} - p^2 \right) \mathcal{B}_0(p^2, m_{u,i}^2, m_{d,j}^2) \right. \\
& + \frac{p^2}{3} + m_{u,i}^2 \mathcal{B}_0(0, m_{u,i}^2, m_{u,i}^2) + m_{d,j}^2 \mathcal{B}_0(0, m_{d,j}^2, m_{d,j}^2) + \frac{(m_{u,i}^2 - m_{d,j}^2)^2}{2p^2} (\mathcal{B}_0(p^2, m_{u,i}^2, m_{d,j}^2) \\
& - \mathcal{B}_0(0, m_{u,i}^2, m_{d,j}^2)) \left. \right] + \frac{2}{3} \left[(2M_W^2 + 5p^2) \mathcal{B}_0(p^2, M_W^2, \lambda^2) - 2M_W^2 \mathcal{B}_0(0, M_W^2, M_W^2) \right. \\
& - \frac{M_W^4}{p^2} (\mathcal{B}_0(p^2, M_W^2, \lambda^2) - \mathcal{B}_0(0, M_W^2, \lambda^2)) + \frac{p^2}{3} \left. \right] + \frac{1}{12s_w^2} \left[((40c_w^2 - 1)p^2 \right. \\
& + (16c_w^2 + 54 - 10c_w^{-2})M_W^2) \mathcal{B}_0(p^2, M_W^2, M_Z^2) - (16c_w^2 + 2)(M_W^2 \mathcal{B}_0(0, M_W^2, M_W^2) \\
& + M_Z^2 \mathcal{B}_0(0, M_Z^2, M_Z^2)) + (4c_w^2 - 1) \frac{2p^2}{3} - (8c_w^2 + 1) \frac{(M_W^2 - M_Z^2)^2}{p^2} (\mathcal{B}_0(p^2, M_W^2, M_Z^2) \\
& - \mathcal{B}_0(0, M_W^2, M_Z^2)) \left. \right] + \frac{1}{12s_w^2} \left[(2M_H^2 - 10M_W^2 - p^2) \mathcal{B}_0(p^2, M_W^2, M_H^2) - 2M_W^2 \mathcal{B}_0(0, M_W^2, M_W^2) \right. \\
& - 2M_H^2 \mathcal{B}_0(0, M_H^2, M_H^2) - \frac{(M_W^2 - M_H^2)^2}{p^2} (\mathcal{B}_0(p^2, M_W^2, M_H^2) - \mathcal{B}_0(0, M_W^2, M_H^2)) - \frac{2p^2}{3} \left. \right] \left. \right\}, \quad (159)
\end{aligned}$$

where the subscripts l , u and d stand for "leptons", "up" and "down" (quarks) respectively. The sum runs over the three generations and λ is the photon mass introduced to regularize the infrared divergencies.

References

- [1] T. Han, J. D. Lykken, and R.-J. Zhang, Phys.Rev. **D59**, 105006 (1999), arXiv:hep-ph/9811350.
- [2] G. F. Giudice, R. Rattazzi, and J. D. Wells, Nucl.Phys. **B595**, 250 (2001), arXiv:hep-ph/0002178.
- [3] C. Corianò, L. Delle Rose, and M. Serino, Phys.Rev. **D83**, 125028 (2011), arXiv:1102.4558.
- [4] M. Giannotti and E. Mottola, Phys. Rev. **D79**, 045014 (2009), arXiv:0812.0351.
- [5] R. Armillis, C. Corianò, and L. Delle Rose, Phys. Rev. **D81**, 085001 (2010), arXiv:0910.3381.
- [6] M. Knecht, S. Peris, M. Perrottet, and E. de Rafael, JHEP **03**, 035 (2004), arXiv:hep-ph/0311100.
- [7] F. Jegerlehner and O. V. Tarasov, Phys. Lett. **B639**, 299 (2006), arXiv:hep-ph/0510308.
- [8] R. Armillis, C. Corianò, L. Delle Rose, and M. Guzzi, JHEP **12**, 029 (2009), arXiv:0905.0865.
- [9] J. Horejsi and M. Schnabl, Z. Phys. **C76**, 561 (1997), arXiv:hep-ph/9701397.
- [10] R. Armillis, C. Corianò, and L. Delle Rose, Phys.Rev. **D82**, 064023 (2010), arXiv:1005.4173.
- [11] W. D. Goldberger, B. Grinstein, and W. Skiba, Phys.Rev.Lett. **100**, 111802 (2008), arXiv:0708.1463.
- [12] A. Denner, Fortschr. Phys. **41**, 307 (1993), arXiv:0709.1075.